Steady Movement of Landslides In Fine-Grained Soils— A Model for Sliding Over an Irregular Slip Surface

U.S. GEOLOGICAL SURVEY BULLETIN 1842–D

AVAILABILITY OF BOOKS AND MAPS OF THE U.S. GEOLOGICAL SURVEY

Instructions on ordering publications of the U.S. Geological Survey, along with the last offerings, are given in the current-year issues of the monthly catalog "New Publications of the U.S. Geological Survey." Prices of available U.S. Geological Survey publications released prior to the current year are listed in the most recent annual "Price and Availability List." Publications that are listed in various U.S. Geological Survey catalogs (**see back inside cover**) but not listed in the most recent annual "Price and Availability List" are no longer available.

Prices of reports released to the open files are given in the listing "U.S. Geological Survey Open-File Reports," updated monthly, which is for sale in microfiche from the USGS ESIC-Open-File Report Sales, Box 25286, Building 810, Denver Federal Center, Denver, CO 80225

Order U.S. Geological Survey publications **by mail** or **over the counter** from the offices given below.

BY MAIL

Books

Professional Papers, Bulletins, Water-Supply Papers, Techniques of Water-Resources Investigations, Circulars, publications of general interest (such as leaflets, pamphlets, booklets), single copies of periodicals (Earthquakes & Volcanoes, Preliminary Determination of Epicenters), and some miscellaneous reports, including some of the foregoing series that have gone out of print at the Superintendent of Documents, are obtainable by mail from

USGS Map Distribution
Box 25286, Building 810
Denver Federal Center
Denver, CO 80225

Subscriptions to periodicals (Earthquakes & Volcanoes and Preliminary Determination of Epicenters) can be obtained ONLY from

Superintendent of Documents
U.S. Government Printing Office
Washington, DC 20402

(Check or money order must be payable to Superintendent of Documents.)

Maps

For maps, address mail order to

USGS Map Distribution
Box 25286, Building 810
Denver Federal Center
Denver, CO 80225

Residents of Alaska may order maps from

U.S. Geological Survey, Map Sales
101 Twelfth Ave., Box 12
Fairbanks, AK 99701

OVER THE COUNTER

Books

Books of the U.S. Geological Survey are available over the counter at the following U.S. Geological Survey offices, all of which are authorized agents of the Superintendent of Documents.

- **ANCHORAGE, Alaska**–4230 University Dr., Rm. 101
- **ANCHORAGE, Alaska**–605 West 4th Ave., Rm G-84
- **DENVER, Colorado**–Federal Bldg., Rm. 169, 1961 Stout St.
- **LAKEWOOD, Colorado**–Federal Center, Bldg. 810
- **MENLO PARK, California**–Bldg. 3, Rm. 3128, 345 Middlefield Rd.
- **RESTON, Virginia**–National Center, Rm. 1C402, 12201 Sunrise Valley Dr.
- **SALT LAKE CITY, Utah**–Federal Bldg., Rm. 8105, 125 South State St.
- **SPOKANE, Washington**–U.S. Courthouse, Rm. 678, West 920 Riverside Ave.
- **WASHINGTON, D.C.**–U.S. Department of the Interior Bldg., Rm. 2650, 1849 C St., NW.

Maps

Maps may be purchased over the counter at the U.S. Geological Survey offices where books are sold (all addresses in above list) and at the following Geological Survey offices:

- **ROLLA, Missouri**–1400 Independence Rd.
- **FAIRBANKS, Alaska**–New Federal Building, 101 Twelfth Ave.

Chapter D

Steady Movement of Landslides In Fine-Grained Soils— A Model for Sliding Over an Irregular Slip Surface

By REX L. BAUM and ARVID M. JOHNSON

Analysis of a possible mechanism for sliding of landslides on irregular slip surfaces shows how surface roughness can retard movement of landslides in fine-grained soils

U.S. GEOLOGICAL SURVEY BULLETIN 1842

LANDSLIDE PROCESSES IN UTAH—OBSERVATION AND THEORY

U.S. DEPARTMENT OF THE INTERIOR
MANUEL LUJAN, JR., Secretary

U.S. GEOLOGICAL SURVEY
Dallas L. Peck, Director

Any use of trade, product, or firm names in this publication is for descriptive purposes only and does not imply endorsement by the U.S. Government

UNITED STATES GOVERNMENT PRINTING OFFICE: 1993

For sale by
USGS Map Distribution
Box 25286, Building 810
Denver Federal Center
Denver, CO 80225

Library of Congress Cataloging-in-Publication Data

Baum, Rex L.
Steady movement of landslides in fine-grained soils : a model for sliding over an irregular slip surface / by Rex L. Baum and Arvid M. Johnson.
p. cm. — (U.S. Geological Survey bulletin ; 1842–D)
(Landslides processes in Utah—observation and theory ; ch. D)
Includes bibliographical references.
Supt. of Docs. no.: I 19.3: 1842–D
1. Landslides—Utah. I. Johnson, Arvid M. II. Title.
III. Series. IV. Series: Landslide processes in Utah—observation and theory ; ch. D.
QE75.B9 no. 1842–D
[QE599.U5]
557.3 s—dc20 92–19448
[551.3'07] CIP

CONTENTS

FIGURES

LIST OF SYMBOLS

A	Amplitude of sine wave
a	A constant
B	Skempton's pore-pressure coefficient
b	A constant
c	Diffusion coefficient
c'	Cohesion of soil in effective stress
$c_1,...c_6$	Constants
E_{xx}, etc.	Strain components
e	Volumetric strain
G	Elastic shear modulus
h	Pressure head at the slip surface, and height of water table above slip surface
H	Static head (pressure head plus elevation head)
K	Hydraulic conductivity
l	Wave number ($2\pi/L$)
L	Wavelength
n	Porosity
n, s	Coordinates normal and tangential to a surface
O	On the order of
P	Pore pressure
q_x, q_z	Specific discharge components
R	Resistance to sliding due to roughness
S	Shear strength of a slip surface
t	Time
T_{xx}, etc.	Stress components
u_x, u_z	Displacement components
v_x, v_z	Velocity components
x, z	Cartesian coordinates
Y_0	Elevation of origin of x-z coordinates above some arbitrary datum
Z	Thickness of a landslide
z_0	Elevation of the wavy slip surface above the x-axis
z_1	Elevation of the ground surface above the x-axis
α	Counterclockwise angle from the x-axis to the horizontal
β	Compressibility of water
γ_t	Unit weight of saturated soil
γ_w	Unit weight of water
η	Viscosity of glacier ice
Θ	Time, in quasi-static coordinate system
θ	Local angle between the x-axis and the wavy slip surface
λ	Counterclockwise angle from the x-axis to a line tangent to the ground surface
μ	Poisson's ratio (drained)
μ_u	Poisson's ratio (undrained)
ξ	$x-\bar{v}_x t$, a coordinate parallel to x-axis
ϕ	Airy's stress function
ϕ'	Friction angle of a soil in effective stress
∇	The divergence operator, $(\partial/\partial x)+(\partial/\partial z)$
∇^2	The Laplacian operator, $\partial^2/\partial x^2+\partial^2/\partial z^2$
∇^4	The biharmonic operator, $\partial^4/\partial x^4+2\partial^4/\partial x^2\partial z^2+\partial^4/\partial z^4$

CONVERSION FACTORS

For the convenience of readers, the metric units used in this report may be converted to inch-pound units by using the following factors:

Multiply metric units	By	To obtain inch-pound units
micrometers (μm)	3.937×10^{-5}	inches
millimeters (mm)	0.03937	inches
centimeters (cm)	0.3937	inches
meters (m)	3.281	feet
pascals (Pa)	0.02089	pounds per square foot
kilopascals (kPa)	20.89	pounds per square foot
kilonewtons per cubic meter (kN/m^3)	6.367	pounds per cubic foot

Steady Movement of Landslides in Fine-Grained Soils—A Model for Sliding Over an Irregular Slip Surface

By Rex L. Baum[1] *and* Arvid M. Johnson[2]

Abstract

Slip-surface roughness can control the velocity of landslides in soils. Field observations indicate that many landslides in soils move by gliding on slip surfaces. Slip surfaces have asperities, including broad steps, depressions, and bumps that can obstruct landslide movement. Landslides typically deform at the asperities in order to stay in contact with the slip surface. Slip-surface asperities can retard the movement of landslides in soils, as asperities retard the movement of temperate glaciers sliding on bedrock surfaces.

An irregular slip surface can control the velocity of a landslide by causing redistribution of pore water near the slip surface. In order to study the effects of this redistribution, we have modeled a landslide, moving over an irregular slip surface, as a porous-elastic solid sliding past a wavy rigid surface. According to our model, water is forced to flow from zones of high pressure at the proximal sides of bumps and is sucked into zones of low pressure on the distal sides of bumps. Resistance to sliding resulting from the irregularity of the surface augments the shear strength of the slip surface. The analysis indicates that the resistance to sliding depends on the roughness of the slip surface, the velocity of the landslide, the hydraulic conductivity of the landslide debris, and the wavelength of the bumps. Other things being equal, landslides in soils having low hydraulic conductivity should move more slowly than landslides in soils having moderate or high hydraulic conductivity.

Our model is consistent with the observations of other workers who found that the velocity of a landslide increases gradually as the water level in the landslide rises. An increasing water level generally results in decreased shear strength at the slip surface. For example, it is known from the infinite slope analysis that the strength of the landslide debris decreases as the water table rises, but the driving force is constant. According to our model, the resistance to sliding (due to roughness of the slip surface) increases to compensate for the loss in strength. For the mechanism of sliding we have analyzed, the resistance due to roughness is proportional to the velocity of the landslide. Thus, as the water table rises, the landslide accelerates until the resistance to sliding over the irregular surface increases sufficiently that it, combined with the strength of the slip surface, balance the driving force.

INTRODUCTION

Surface roughness has been recognized as a source of sliding resistance in rock slopes (Patton, 1966), glaciers (Kamb, 1970) and faults (Byerlee, 1970). However, surface roughness has only recently been recognized as a source of significant sliding resistance for landslides in soils (Baum, 1988; Dounias and others, 1988; Mizuno, 1989). The basal and lateral slip surfaces of landslides in soils are irregular; they have bumps, steps, depressions, and other features. The roughness of these surfaces can retard movement of a landslide so as to control its velocity.

Observations show that many landslides move for weeks, months, or even longer at rates ranging from less than a millimeter per day to a few meters per day. Keefer and Johnson (1983, p. 44, 45) compiled data from many sources on the maximum and average velocities of landslides in soils. The average velocities range from 10^{-5} to 10 m/d (meters per day), and the maximum velocities range from 10^{-3} to 10^{4} m/d (maximum velocities ranging from 10^{2} to 10^{4} m/d were attained during surges).

Landslides commonly move at constant rates for periods of several days. These periods are interrupted by shorter periods (lasting perhaps several minutes) of acceleration and deceleration. However, sustained acceleration resulting in very rapid movement rarely occurs (Keefer and Johnson, 1983, p. 46–48).

Steady movement of landslides cannot be explained in terms of slope stability theory, which predicts that a landslide will accelerate indefinitely as soon as the driving forces exceed the frictional and cohesive resisting forces on the slip surface (Keefer and Johnson, 1983, p. 48, 49). For example, according to slope-stability theory, a slight increase of pore-water pressure at the slip surface of a landslide at limiting

Approved for publication February 26, 1992.

[1]U.S. Geological Survey, Box 25046, MS 966, Denver, CO 80225.
[2]Dept. of Earth and Atmospheric Sciences, Purdue University, West Lafayette, IN 47907.

equilibrium ought to cause the landslide to accelerate without bound.

Field measurements show that velocities of landslides increase gradually with increasing pore-water pressures. Terzaghi (1950, p. 120) observed a linear relationship between water level and velocity in a landslide that was about 40 m deep. The velocity increased from about 60 mm/d when the water level was 3.0 m below the ground surface to about 200 mm/d when the water level was only 1.0 m below the ground surface. Rybář (1968, p. 140) observed that a landslide, 5.4 m deep, accelerated from rest to about 8 mm/d as water levels increased by 1 m. The velocity of a landslide in Japan increased from about 1 mm/d to 13 mm/d as the water level in a borehole rose about 2 to 2.5 m (Japan Society of Landslide, 1980, p. 9). Similar findings were reported by Iverson (1986).

A popular model used to explain the steady movement of landslides is inconsistent with some field observations. In the model, the velocity at the basal boundary of the landslide is assumed to be zero, and flow of soil is assumed to occur in a layer of material above the basal boundary (Ter-Stepanian, 1965; Yen, 1969; Keefer, 1977; Suhayda and Prior, 1978; Craig, 1981; Savage and Chleborad, 1982; Iverson, 1986; and others). This model is usually justified on the basis of inclinometer profiles; however, deformation of an inclinometer tube might not bear a close resemblance to the deformation of the soil containing the tube. In fact, field observations (Keefer and Johnson, 1983; Hutchinson, 1970; Prior and Stephens, 1972; Niigata Laboratory, 1973) indicate that the main body of a landslide moves primarily by sliding. Furthermore these observations show that the velocity at the basal slip surface nearly equals the velocity at the ground surface, and deformation is concentrated near the slip surface.

A possible explanation for the steady movement of landslides in soils is that strength of material at the slip surface is velocity dependent, although this explanation is discounted by several investigators. Keefer and Johnson (1983) determined that the shear strength of a sample of landslide slip surface increased linearly with the log of the velocity, so that the strength of the material tested increased only 2.5 percent for each tenfold increase in velocity. They concluded that such an increase is too small to account for the steady movement of landslides. Similar results were obtained by Kenney (1968), Ramiah and Purushothamaraj (1971), and Mitchell (1976, p. 292), who indicate that shear strength of soils generally increases 5 to 10 percent for each tenfold increase in rate of deformation. Recently, however, Skempton and others (1989) have argued that this small velocity dependence of the strength could explain the movements of the Mam Tor landslide in England.

In this study, we investigated how roughness might control the rate of movement of a landslide that moves mainly by sliding on a basal slip surface as an alternative to models that attempt to explain steady movement by means of viscous flow or rate-dependent shear strength.

Similarities between the movement of glaciers and the movement of landslides in soils indicate that the mechanisms that control the rate of sliding of temperate glaciers may be analogous to that of landslides (Keefer and Johnson, 1983, p. 53). Both glaciers and landslides move slowly and steadily, and some temperate glaciers are known to move by sliding over irregular bedrock surfaces (Kamb and LaChapelle, 1964). Surface roughness (unevenness of the bedrock surface) has been shown to retard movement of temperate glaciers; regelation and plastic deformation of the ice make sliding on the rough surfaces possible (Kamb and LaChapelle, 1964; Lliboutry, 1968; Budd, 1970a; Kamb, 1970; Nye, 1969, 1970; Morland, 1976a, 1976b). In regelation, water moves around asperities by melting of ice at the proximal sides and refreezing at the distal sides of asperities. The rate of regelation is controlled by the rate of heat transfer in the ice and in the bedrock. In plastic deformation, solid ice flows around asperities. The rate of plastic deformation is controlled by the rheological properties of the ice.

Similarly, surface roughness could retard movement of landslides. Sliding over a rough surface might cause movement of pore fluid, due to consolidation and swelling, as well as plastic deformation of landslide debris. Consolidation at the proximal sides and swelling at the distal sides of asperities might play a role corresponding to that of regelation in glaciers. The rate of consolidation and swelling is controlled by the movement of water, which is related to the permeability of the soil. Henceforth, this mechanism is called *forced circulation*, because volume change of the soil forces water to circulate from places of high pressure to places of low pressure. Plastic deformation around the obstacles might be distributed as plastic flow, or localized on slip surfaces that form within the landslide debris. In either case, plastic deformation will resist sliding. No matter what the mechanism of deformation during sliding, the asymmetric pressure distribution that occurs at the slip surface during sliding results in a net force opposing sliding of the soil. Mizuno (1989) analyzed a possible mechanism of plastic deformation by assuming that deformation in an active landslide is analogous to deformation that occurs during undrained triaxial creep tests, and derived an equation for predicting the velocities of landslides in clayey soils. Forced circulation of pore fluid around asperities is the model investigated here, as an alternative rate-dependent process to explain the steady movement of landslides. We cannot couple forced circulation and plastic flow in a simple way, and we have neglected plastic deformation in order to make our analysis as simple as possible.

Acknowledgments

Robert Fleming of the U.S. Geological Survey (USGS) shared useful insights and criticism as we were writing this paper. William Z. Savage, Richard M. Iverson, and David J. Varnes (all USGS) provided critical reviews

that resulted in improvements. David J. Varnes shared ideas and references needed to help document the fact that landslides in soils move by sliding on slip surfaces.

SLIP SURFACES IN LANDSLIDES

The analogy we proposed between the mechanisms that control the rate of movement of landslides and the mechanisms that control the rate of movement of some temperate glaciers is reasonable if landslides move by gliding over irregular surfaces, as do the glaciers. We describe slip surfaces of landslides in clayey soils in order to show that the slip surfaces of many such landslides could be sufficiently bumpy to retard landslide movement.

Slip surfaces in clayey materials form in thin layers of parallel clay particles where deformation has been concentrated. Hutchinson (1983, p. 243) noted that layers containing slip surfaces are often paper thin, making them difficult to locate in samples and exploratory trenches. Mary Riestenberg (College of Mount St. Joseph, oral commun., 1987) observed that the slip surfaces of shallow landslides in Cincinnati occur in paper-thin layers. Observations made using a polarizing microscope (Skempton and Petley, 1968; Morgenstern and Tchalenko, 1968) indicate that slip surfaces are in layers of strongly oriented clay particles from 100 to 500 micrometers thick. Typically, the clay within a few centimeters of the slip surfaces is deformed or remolded, but deformation is concentrated on the slip surfaces.

The existence of slip surfaces in landslides has been recognized for more than a century. Collin (1846) was the first to document and accurately describe slip surfaces of landslides that occurred in clay embankments and cuts in clay slopes. During the course of repairing the landslides, the debris was cleared away, exposing the basal slip surfaces. They were "smooth, slippery and soapy" surfaces.

Summarizing observations of many landslides, Skempton and Petley (1968, p. 33) indicated that slip surfaces occur in the majority of landslides. They indicate that slip surfaces extend over large areas beneath a landslide and are polished subplanar surfaces, striated parallel with the direction of movement.

Observations and measurements indicate that landslides move primarily by gliding on their slip surfaces. Collin (1846, p. 36, 37) was able to show that the basal slip surfaces formed as a result of landslide movement and that movement occurred primarily by sliding on the basal slip surface. He observed that the bedding or layering was tilted and offset across the basal slip surface of a landslide.

A sequence of time-lapse photographs by the Niigata Laboratory (1973) shows that displacement of the Sarukuyoji landslide occurred primarily on a slip surface. The photographs show the face of a trench in the landslide. At time zero, no slip surface is visible, but after five minutes, the trace of the slip surface is visible as a faint line across the face of trench. After 35 minutes, the shadow cast by the overhanging edge of the block of soil above the slip surface makes a broad black stripe across the photograph. The photographs show clearly that the movement of the landslide is concentrated on a slip surface. The photographs show no evidence that any other deformation occurred at the face of the trench during the 35-minute period.

Similarly, photographs of the face of a pipeline trench show that sliding occurred on a surface (fig. D1). The light band of soil in the middle of figure D1*A* contains the slip surface. Colluvium overlying the slip surface slid 1–2 mm downslope after the trench was opened, and the shadow of the overhanging material (narrow black line through the center of the white band of soil in figure D1*B*) clearly shows that deformation was concentrated at the slip surface.

At a shallow earthflow in California, experiment showed that deformation was concentrated on the basal slip surface (Keefer and Johnson, 1983, p. 31, 32). A stack of wooden disks, shaped like poker chips, was placed in a borehole that penetrated the basal slip surface of the main body of the landslide. After the landslide had moved about 0.4 m, the disks were recovered by digging a trench next to the borehole, and the positions of the disks were mapped. At least 94 percent of the movement occurred within 1.3 cm (the thickness of one disk) of the basal slip surface. Little evidence of deformation outside the slip surface was observed.

Ter-Stepanian (1965, p. 577) performed a similar experiment with wooden blocks, each 0.2 m high, stacked in a borehole. The profile of the blocks was exposed in a trench after 5 yr of movement. Total displacement at the ground surface was 2.8 m. The block just above the basal slip surface (3.8 m deep) was displaced 2.2 m. The upper 3 m of the stack of blocks leaned several degrees downslope, and blocks in the lower 0.8 m of the stack were offset or rotated. Although part of the displacement was due to internal deformation of the landslide debris, most of the displacement (78 percent) was concentrated on the basal slip surface.

Displacement at the lateral boundaries of many landslides also occurs on slip surfaces. Strike-slip faults having slickensided surfaces constituted the lateral boundaries of the Aspen Grove landslide in central Utah. Displacement measurements at three transverse lines of stakes on the landslide showed that displacement at the boundaries was from 85 to 95 percent of the displacement at the axis of the landslide. David Varnes (USGS, oral commun., 1988) reported similar findings for the Slumgullion landslide in southern Colorado.

Several investigators have reported that some deep landslides move on "thick kneaded zones," layers of clay, several decimeters thick, that have been strongly sheared and remolded (Zaruba and Mencl, 1982, p. 161; Gould, 1960; Brunsden, 1984). However, even the kneaded zones are bounded by or contain slip surfaces that accommodate most

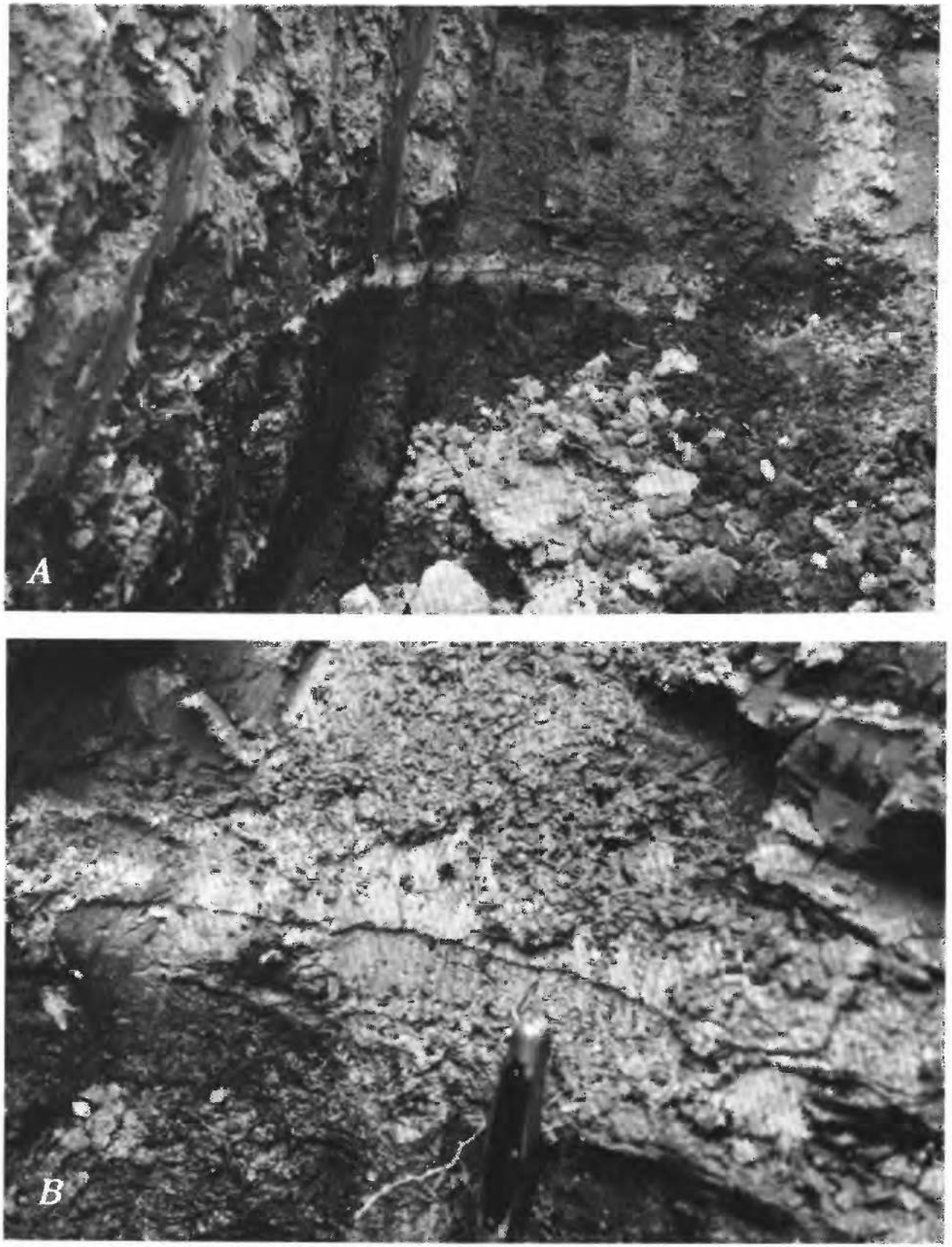

Figure D1. Displacement on a slip surface exposed in a pipeline trench in West Virginia. (*A*) Overview showing location of slip surface (in white layer of clay) in the side of the trench. (*B*) Close-up of slip surface. Displacement of overhanging block toward the camera shown by shadow across middle of light-colored layer of clay. Knife handle in both photographs is 9 cm long. (Photographs by Robert W. Fleming, U.S. Geological Survey.)

of the displacement. A horizontal layer of black plastic clay (1 m thick, thinly laminated and schistose) within less plastic, stony, brown colluvium, was exposed at the base of the eroded toe of the Twin Lake landslide (about 30 m deep), near Mayfield, Utah. The black clay, evidently part of the basal slip zone of the landslide, was divided into almond-shaped pieces by a family of anastomosing, subhorizontal slip surfaces. A layer of "kneaded" clay exposed in a landslide in the south bank of Ephraim Creek, near Ephraim, Utah, was bounded at its top by slip surfaces (fig. D2). Several meters away, at another exposure, polished slip surfaces formed the boundaries between layers of plastic clay and the gravel-rich colluvium that they had intruded (figs. D3*A* and *B*). Thus, movement by gliding on slip surfaces appears to be almost universal in landslides.

Slip Surface Irregularities

Slip surfaces deviate from the idealized cylindrical or planar shapes assumed in most stability analyses. Steps, bumps, depressions, grooves, striations, and other irregularities have been observed on slip surfaces of landslides in California, Utah, France, Norway, and Japan (Collin, 1846; Stout, 1971; Mizuno, 1989).

Striations and grooves are commonly observed on slip surfaces (fig. D4). They form as a result of deformation at small irregularities in the slip surface that might retard landslide movement slightly. Striations and grooves are parallel to the direction of movement of the landslide, so they cannot cause significant deformation of the landslide debris; rather, they merely increase the area of the slip surface.

Steps, depressions, and bumps are other types of irregularities on a slip surface and they can obstruct movement. Such irregularities are termed asperities. Asperities are oblique to the direction of movement so that they can cause interlocking or deformation (either distributed or localized on faults) of the landslide debris. (See Savage and Smith, 1986, for a discussion of one style of deformation that can occur in landslides.)

Slip surfaces of some landslides in France had streamlined bumps that caused them to deviate from idealized cycloidal shapes (Collin, 1846, pl. VI, VII, VIII, and others). Accurate surveys showed that the bumps were a few meters long and a few decimeters high.

The slip surfaces of two landslides in California had steps that consisted of rounded treads (flats) and risers (ramps) (Stout, 1971). The treads had slopes as low as 4°, and the risers had slopes as steep as 41°. The average slope

Figure D2. Cross-sectional view of a shear (or kneaded) zone exposed in bank of Ephraim Creek near Ephraim, Utah. Dark lens-shaped area, *A*, is part of a slip surface exposed in an overhang and is approximately 30 cm across.

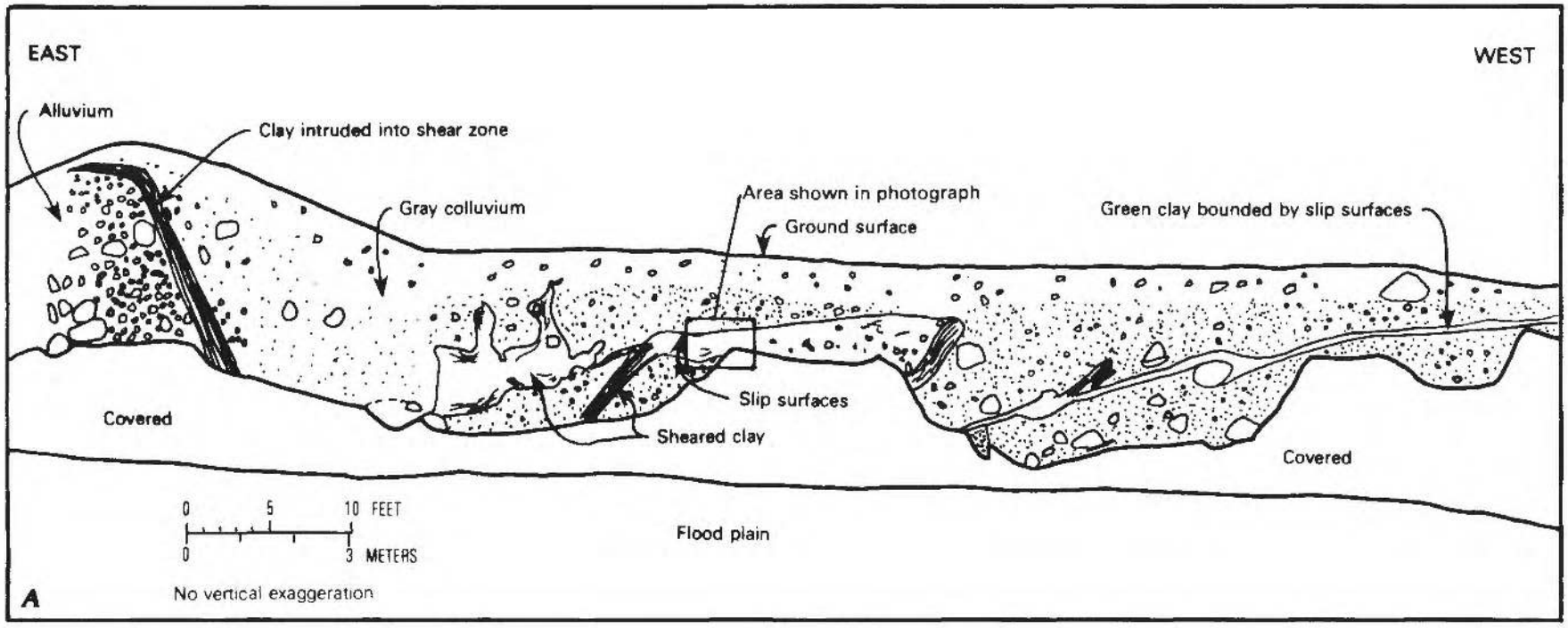

Figure D3. Shear zones and intruded layers of clay exposed in the bank of Ephraim Creek. (*A*) Sketch of bank along creek. (*B*) Close-up of clay layer shown in sketch. Layer is bounded both above and below by slip surfaces, which are marked by horizontal scale (15 cm long) and trowel handle.

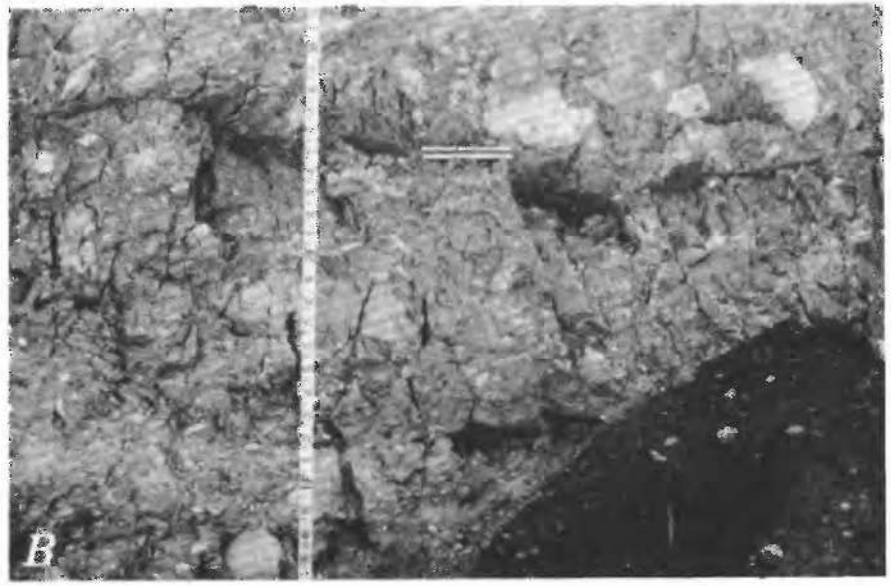

Figure D4. Slip surface on a thrust fault within the Thistle landslide, Thistle, Utah. The slip surface is covered with grooves and striations. (Photograph by Irving J. Witkind, U.S. Geological Survey.)

of each slip surface was about 14°. Measured relative to a smoothly curving, average slip surface, the steps were from 3 to 6 m high and tens of meters long (fig. D5).

Steps were also observed in the basal slip surface of a quick-clay landslide in Norway (Stout, 1971). About one third of the slip surface was exposed, including parts of the steps. The steps had rounded noses that separated broad, gently sloping treads from steep risers. The treads sloped about 0.5° to 2.0°, and the risers sloped as steeply as 50°. The risers were from 5 to 7 m high, and the average slope of the slip surface (not including the headscarp) was about 5°.

Streamlined bumps are common on the slip surface of the Indianola landslide in central Utah. The slip surface is roughly a U-shaped (fig. D6*A*) or V-shaped (fig. D6*B*), slightly sinuous channel. Grooves and striations on the sides of the channel are approximately parallel to the channel bottom (figs. D6*A* and *B*). Larger bumps on the sides of the channel are a few meters long and small bumps, each less than a meter long, are superimposed on the larger bumps (fig. D6*A*). Many of the smaller bumps are relatively narrow features oriented approximately parallel to the direction of movement.

Elongate, asymmetrical ridges resembling roches moutonnées are exposed in a lateral slip surface of a landslide at Cottonwood Spring in Ephraim Canyon, Utah (fig. D7). All are 15 to 40 cm long, 5 to 15 cm wide, and a few centimeters high, and are superimposed on a larger bump that is about 1 to 1.5 m long. There are other larger bumps nearby.

To summarize, several general observations can be made about slip surfaces of landslides. The main body of a landslide moves principally by sliding on a single slip surface within a thin (usually less than 1 mm thick) layer of strongly oriented clay particles. In many landslides, from at least 90 to 95 percent of the displacement observed at the ground surface occurs on the basal slip surface; minor deformation occurs in the ground adjacent to the slip surface of the main body of a slide; however, significant deformation may occur throughout the thickness of the slide in the vicinity of the head, toe, and major asperities in the failure surface.

Slip surfaces of landslides in clayey materials are irregular. Asperities on slip surfaces comprise bumps that resemble flattened domes or roches moutonnées, broad steps having steep risers and gently sloping treads, and perhaps other forms. Lengths of asperities range from decimeters to tens of meters. Generally, the amplitudes or heights are small compared to the lengths of the asperities. Mizuno (1989) reports that the average ratio of height to length is 0.065. Asperities tend to be asymmetrical; distal slopes are generally steeper than proximal slopes.

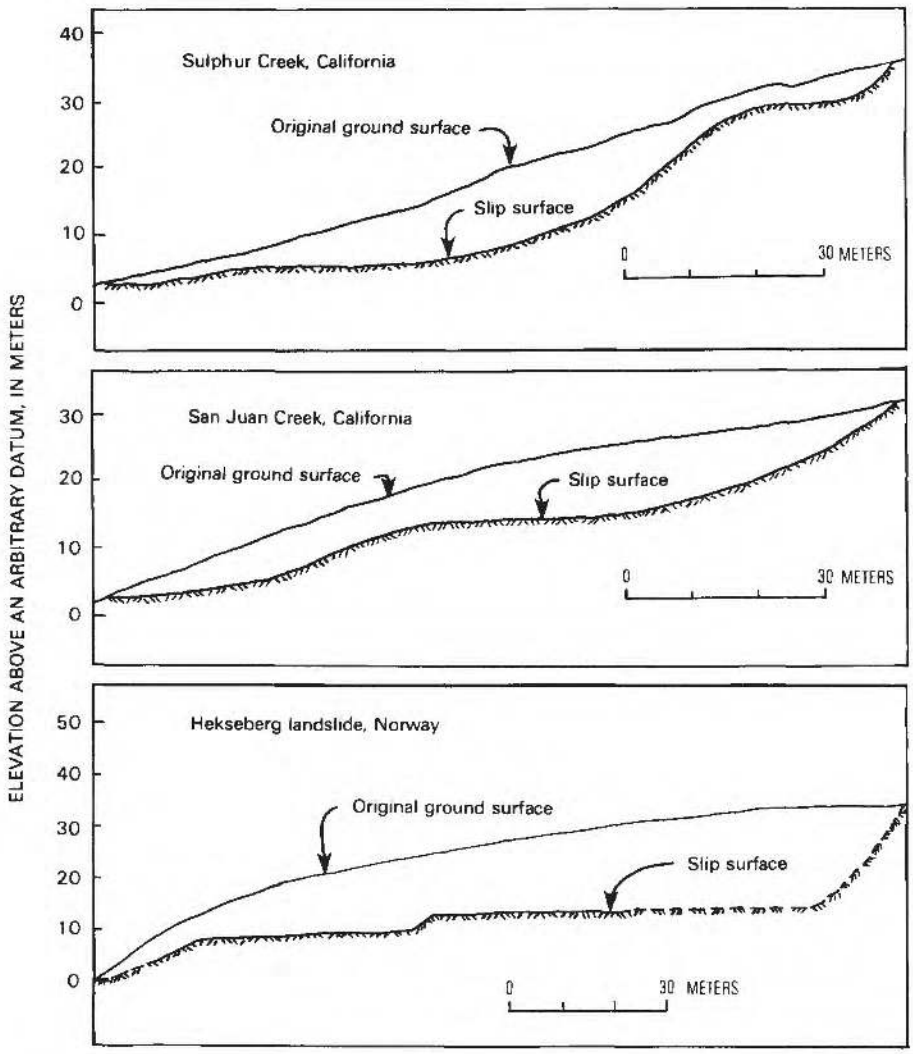

Figure D5. Profiles of stepped slip surfaces of landslides. (Modified from Stout, 1971.)

EQUILIBRIUM OF A LANDSLIDE MASS ON AN IRREGULAR SLIP SURFACE

Resistance to sliding on an irregular slip surface is determined by the stresses acting on the landslide mass (fig. D8). In the following derivation we separate sliding resistance into a shear stress and a normal stress acting on an irregular slip surface. The normal stress that acts on the irregular slip surface can oppose sliding, as does the shear stress of the slip surface. To demonstrate this, we integrate the differential equation for equilibrium in the x-direction,

$$\frac{\partial T_{xx}}{\partial x} + \frac{\partial T_{zx}}{\partial z} + \gamma_t \sin\alpha = 0 \qquad (1a)$$

(See "List of symbols" on p. IV for definitions of terms.) We assume that normal stresses are positive in tension (the notation for stresses is after Malvern, 1969). Following the methods used by several glaciologists (Collins, 1968; Budd, 1970b; and Kamb, 1986), we integrate with respect to z, between the elevation of the basal slip surface, $z=z_0(x)$, and the elevation of the ground surface, $z=z_1(x)$:

$$\int_{z_0}^{z_1} \frac{\partial T_{xx}}{\partial x} dz + \int_{z_0}^{z_1} \frac{\partial T_{zx}}{\partial z} dz + \int_{z_0}^{z_1} \gamma_t \sin\alpha \; dz = 0. \qquad (1b)$$

In equations 1a and 1b, the unit weight of soil, assumed constant with respect to x and z, is γ_t, and the counterclockwise angle from the x-axis to the horizontal is α. We have used the convention that normal stresses are positive in tension. T_{xx} is the normal component of stress acting parallel to x, and T_{zx} is the shear stress acting parallel to x.

Equation 1b is related to integrated forms of the equilibrium equation used to study longitudinal stress and strain gradients in glaciers (Collins, 1968; Budd, 1970b; Kamb, 1986). However, the following analysis differs in that we work with the total stresses, whereas the glaciologists cast

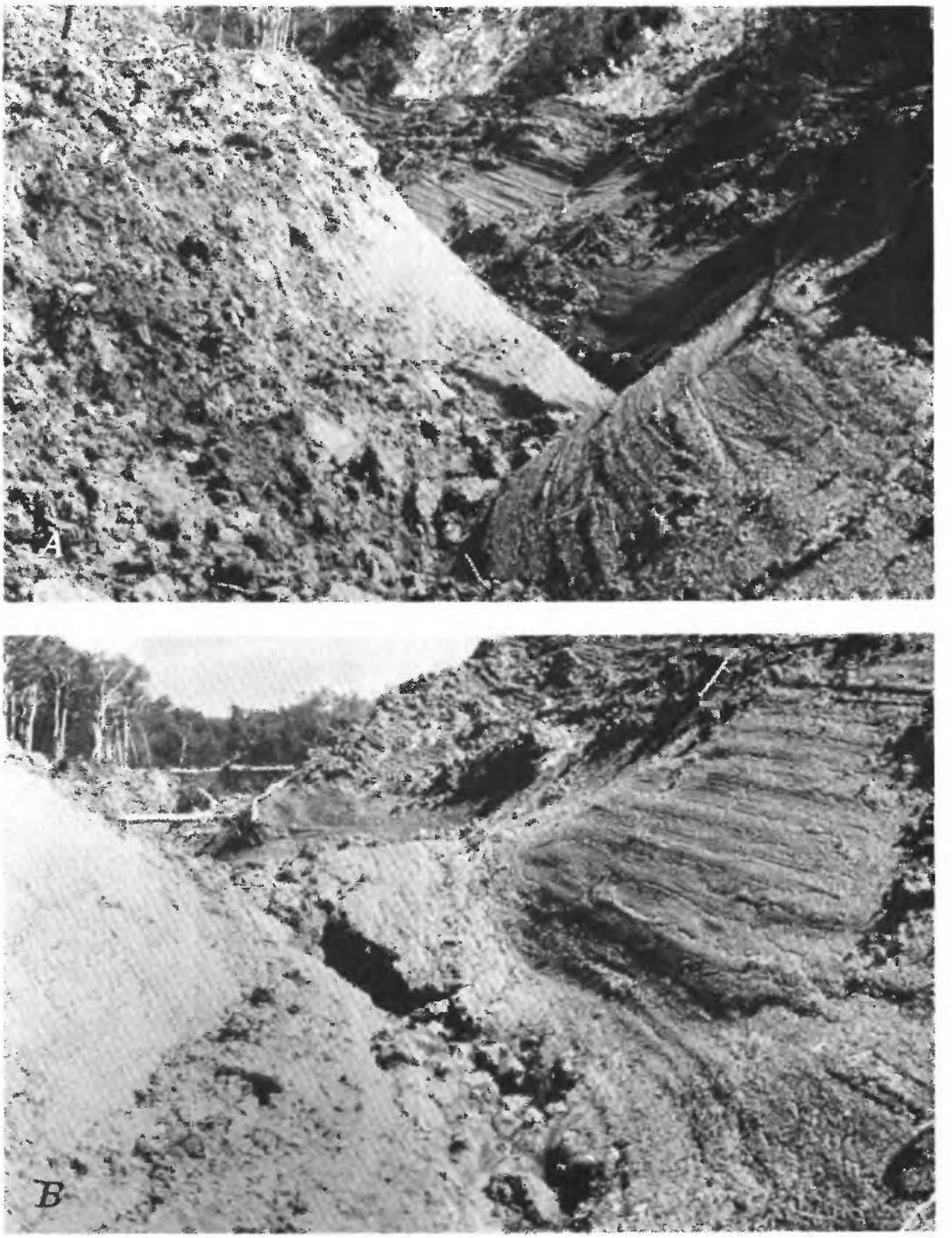

Figure D6. Slip surface of a landslide near Indianola, Utah. (*A*) The landslide occupied a V-shaped channel or trough. Striations on channel wall are parallel to the transport direction. Elongated bumps are transverse to direction of movement. (*B*) Curvature of channel and rounded shapes of bumps on the slip surface are evident in this view.

Figure D7. A lateral slip surface of the Cottonwood Spring landslide, Ephraim Canyon, Utah. Features resembling roches moutonnées are visible near center of photograph. Lens cap is about 5 cm in diameter. Arrow shows direction of landslide movement.

their equations in terms of deviatoric stresses. This is because the flow of glacier ice is considered to be independent of the hydrostatic or mean stress (Collins, 1968), whereas deformation of landslide debris is known to depend on the mean stress (Lambe and Whitman, 1969). Consequently, equation 1b is closely related to one of the equations of equilibrium used in stability analysis of landslides (Morgenstern and Price, 1965; Janbu, 1973). Mizuno (1989) also analyzed equilibrium on a wavy slip surface; however, his derivation differs from ours in several ways, so his results cannot be readily applied to part of our analysis.

When we evaluate the last two integrals in equation 1b, the equation simplifies to

$$\int_{z_0}^{z_1} \frac{\partial T_{xx}}{\partial x} dz + [T_{zx}]_{z_1} - [T_{zx}]_{z_0} + \gamma_t (z_1 - z_0) \sin\alpha = 0. \tag{1c}$$

Note that the second term in equation 1b integrates readily (Wylie and Barrett, 1982, p. 795–797).

The remaining integral in equation 1b can be evaluated by means of Leibnitz's rule,

$$\int_{z_0}^{z_1} \frac{\partial T_{xx}}{\partial x} dz = \frac{d}{dx} \int_{z_0}^{z_1} T_{xx} dz - [T_{xx}]_{z_1} \frac{dz_1}{dx} + [T_{xx}]_{z_0} \frac{dz_0}{dx}. \tag{1d}$$

In equation 1d, dz_1/dx and dz_0/dx denote the slope (dz/dx) of a line tangent to the ground surface, or slip surface, respectively.

We substitute equation 1d into 1c, and move terms evaluated at the slip surface, $z=z_0$, to the right side of the equation,

$$\frac{d}{dx} \int_{z_0}^{z_1} T_{xx} dz + \gamma_t (z_1 - z_0) \sin\alpha + [T_{zx}]_{z_1} - [T_{xx}]_{z_1} \frac{dz_1}{dx} = [T_{zx}]_{z_0} - [T_{xx}]_{z_0} \frac{dz_0}{dx}. \tag{1e}$$

We assume that the stresses acting normal, T_{nn}, and tangential, T_{ns}, to the ground surface are zero. Equilibrium

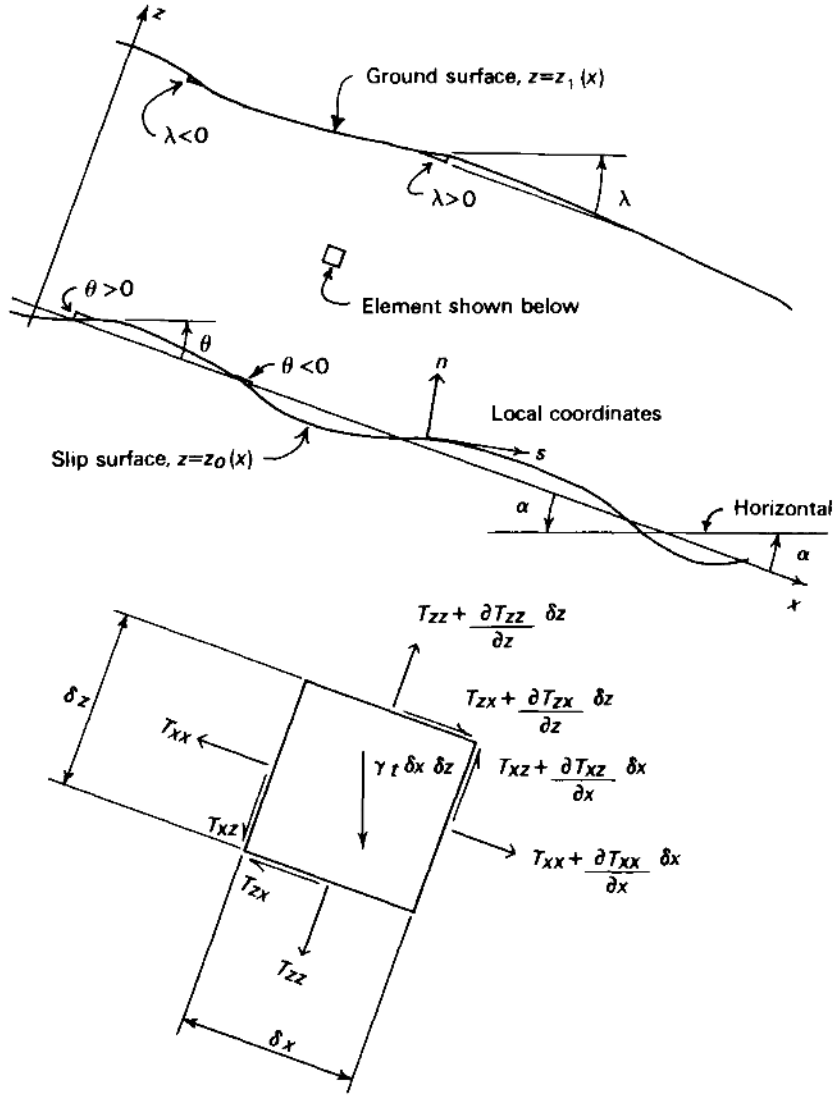

Infinitesimal element, showing variation of stress within the landslide

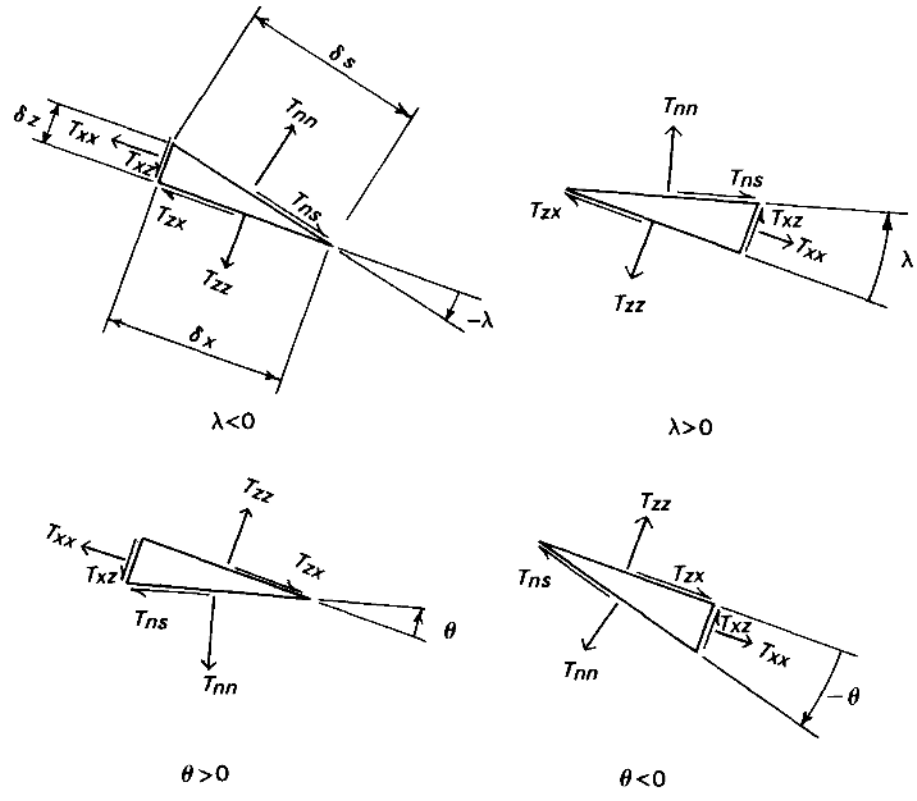

Elements for transforming stresses from *x*-*z* coordinates to *n*-*s* coordinates at a point

Figure D8. Stresses acting at the ground surface, at the slip surface, and within a typical landslide. The *x*-axis is along the average slope of the slip surface; α is the acute angle measured from the *x*-axis to the horizontal. The *z*-axis is normal to *x*. Local coordinates *n* and *s* are normal and tangential to the slip surface, respectively. The slope of the ground surface, with respect to the *x*-axis, is dz_1/dx, or $\tan \lambda$; λ is the angle measured counterclockwise from the *x*-axis to a line tangent to the ground surface. Likewise, the slope of the slip surface with respect to the *x*-axis is dz_0/dx, or $\tan \theta$; θ is the angle measured counterclockwise from the *x*-axis to a line tangent to the slip surface at any point *x*. All stresses acting on elements of the landslide debris are shown in their positive orientations.

parallel to the x-direction at the ground surface (fig. D8, stresses for $\lambda>0$) requires that

$$[T_{ns}]_{z_1}\,\delta s\,\cos\lambda-[T_{nn}]_{z_1}\,\delta s\,\sin\lambda = [T_{zx}]_{z_1}\,\delta x - [T_{xx}]_{z_1}\,\delta z. \quad (2a)$$

In equation 2a, δs, δx, and δz are small increments parallel to s, x, and z, respectively. Note that $\delta x/\delta s=\cos\lambda$ and $\delta z/\delta s=\sin\lambda$ in the limit as δs, δx, and δz become infinitesimals. We divide equation 2a by $\delta s\cos\lambda$ to obtain

$$[T_{ns}]_{z_1} - [T_{nn}]_{z_1}\tan\lambda = [T_{zx}]_{z_1} - [T_{xx}]_{z_1}\tan\lambda. \quad (2b)$$

In equation 2b, $\tan\lambda$ equals (dz_1/dx), in the limit as δx becomes infinitesimal. The reader can verify that equation 2b is correct, whether λ is greater or less than zero, by observing how the normal stresses change their orientation as λ changes sign. All stresses shown in figure D8 are positive, according to the sign convention adopted previously. For $\lambda>0$ ($\tan\lambda>0$), the x-components of the normal stress act in the opposite direction to the x-components of the corresponding shear stresses. For $\lambda<0$ (and $\tan\lambda<0$), the x-components of the normal stresses act in the same direction as the x-components of the corresponding shear stresses (fig. D8).

The left side of equation 2b is zero because the stresses at the ground surface, $[T_{nn}]_{z_1}$ and $[T_{ns}]_{z_1}$, are zero. By substituting this result into equation 1e, we determine that

$$\frac{d}{dx}\int_{z_0}^{z_1} T_{xx}dz + \gamma_t(z_1-z_0)\sin\alpha = [T_{zx}]_{z_0} - [T_{xx}]_{z_0}\frac{dz_0}{dx}. \quad (3)$$

Equation 3 is an exact statement of the requirements for equilibrium at any position along the slip surface. We need an expression for the overall equilibrium of the landslide mass. If we assume that the waviness of the slip surface of the landslide is periodic, with wavelength L;, that the ground surface is stress-free and parallel to the x-axis; and that the slope has an infinite extent, then we can derive such an expression by integrating equation 3 with respect to x, over one wavelength, L, and dividing by L,

$$\frac{1}{L}\int_0^L \frac{d}{dx}\int_{z_0}^{z_1} T_{xx}dz\;dx + \frac{1}{L}\int_0^L \gamma_t(z_1-z_0)\,(\sin\alpha)\,dx = \frac{1}{L}\int_0^L [T_{zx}]_{z_0}dx - \frac{1}{L}\int_0^L [T_{xx}]_{z_0}\frac{dz_0}{dx}dx. \quad (4a)$$

The first term on the left side of equation 4a is zero. The gradient of longitudinal force per unit width, $\frac{d}{dx}\int_{z_0}^{z_1} T_{xx}dz$ (the integrand of the first term), is a periodic function of x. The average value of the gradient, $\frac{1}{L}\int_0^L \frac{d}{dx}\int_{z_0}^{z_1} T_{xx}dz\,dx$, must be zero so that the longitudinal force per unit width does not become infinite at large values of x. For example, if the average value of the gradient were a (non-zero) constant, then the absolute value of the longitudinal force would increase without bound in proportion to x. The second integral on the left side can be evaluated explicitly, so that equation 4a simplifies to

$$\gamma_t Z\,\sin\alpha = \frac{1}{L}\int_0^L [T_{zx}]_{z_0}dx - \frac{1}{L}\int_0^L [T_{xx}]_{z_0}\frac{dz_0}{dx}dx. \quad (4b)$$

In equation 4b, Z is the average thickness of the landslide mass. For convenience, we let

$$R = \frac{1}{L}\int_0^L [T_{xx}]_{z_0}\frac{dz_0}{dx}dx. \quad (4c)$$

Equation 4b is an expression for overall equilibrium of an infinite slope having a wavy, periodic slip surface. It shows that the average shear stress due to weight of the landslide debris (left side of equation 4b) is balanced by the average shear stress at the slip surface (first term on right side of equation 4b) and the average resistance (acting parallel to x) due to roughness of the slip surface, R. If the slip surface is perfectly smooth, such that $(dz_0/dx)=0$, then the second integral on the right side of equation 4b, R vanishes, and the equation reduces to the well-known expression of equilibrium for an infinite slope. Thus, R can be thought of as a correction term for the effect of roughness.

Roughness can increase the resistance to sliding only if the material above the slip surface is stronger than the slip surface. Baum (1988) has shown analytically, for a von Mises plastic, that resistance to sliding is greater on a rough (bumpy) slip surface than on a smooth one, provided that the strength of the material is greater than the adhesion of the material to the slip surface. Laboratory experiments, in progress (Baum, unpub. data) corroborate this analysis. However, if strength of the material equals the adhesion to the rough slip surface, then sliding must occur on a smooth surface within the material because the resistance to sliding on the rough surface will exceed the strength of the material.

Roughness of the slip surface contributes to equilibrium of a landslide mass because the distribution of normal force on the slip surface is asymmetrical. The compressive normal stress, T_{xx}, is greater (in absolute value) on the proximal sides of bumps than on the distal sides. The resultant force due to the action of the normal stress on the bumps opposes downslope movement of the landslide mass.

Thus, in a landslide, normal stress on the slip surface contributes to equilibrium in two distinct ways. First, it contributes to equilibrium by determining the shear strength, S, as indicated by the Coulomb-Terzaghi yield criterion,

$$S = c' - \{ [T_{nn}]_{z_0} + [P]_{z_0} \} \tan\phi'. \qquad (5a)$$

and second, it contributes to equilibrium through roughness. In equation 5a, P is the pore pressure (negative in tension), c' is the cohesion for effective stress and tan ϕ' is the coefficient of friction for effective stress. We assume, hereafter, that the average shear stress at the slip surface equals the average shear strength when the landslide is active.

The two contributions of normal stress to equilibrium can be seen clearly in the equation of equilibrium by transforming stresses at the slip surface in equation 4b to local coordinates tangent and normal to the slip surface, and by substituting the yield criterion for the slip surface (equation 5a) into equation 4b. The equation for transformation of stress to local coordinates (see fig. D8 and equations 2a and 2b) is

$$[T_{ns}]_{z_0} - [T_{nn}]_{z_0} \frac{dz_0}{dx} = [T_{zx}]_{z_0} - [T_{xx}]_{z_0} \frac{dz_0}{dx}. \qquad (5b)$$

Equations 5a and 5b are substituted into equation 4b to show the two ways that normal stress at the slip surface contributes to equilibrium

$$\gamma_t Z \sin\alpha = \frac{1}{L}\int_0^L (c' - \{ [T_{nn}]_{z_0} + [P]_{z_0} \} \tan\phi') dx - \frac{1}{L}\int_0^L [T_{nn}]_{z_0} \frac{dz_0}{dx} dx. \qquad (5c)$$

The first term on the right side of equation 5c determines the shear strength, and the second term determines the resistance to sliding due to roughness. Significantly, the effective normal stress (T_{nn}+P) enters the shear strength term, whereas the total normal stress enters the roughness term.

The contribution of normal stress to equilibrium, through the roughness of the slip surface, may seem unfamiliar to some readers. Perhaps it can be visualized by considering the action of one gear driving another gear in a machine. Torque is transferred from one gear to the other through the normal stresses acting on the faces of gear teeth that are in contact. The gears are lubricated so that shear stress on the faces of the teeth is small. Compressive normal stress on the leading faces of these gear teeth is greater than on the trailing faces. This asymmetrical distribution of stress on the gear teeth is similar to the asymmetrical stress distribution that we expect to occur at asperities on the slip surface of a landslide.

THE ROLE OF FORCED CIRCULATION IN THE EQUILIBRIUM OF A LANDSLIDE

Within the framework of the general theory of slope equilibrium just described, we wish to focus on a possible mechanism that can explain the observed rate dependence of the forces that resist sliding. We have already noted that the rate dependence of the shear strength of slip surfaces is too weak to explain the steady movement of landslides, because the shear strength increases only about 5–10 percent for each tenfold increase in the rate of shearing, within the range of rates tested (Kenney, 1968; Ramiah and Purushothamaraj, 1971; Mitchell, 1976; Keefer and Johnson, 1983). Thus, to explain the steady movement, we examine a possible mechanism of sliding in which R is rate dependent.

The mechanism we propose, in order to explain the rate dependence of R, is forced circulation of pore fluid through the landslide debris. As the landslide moves over its bumpy slip surface, high compressive normal stress on the proximal sides of bumps forces fluid to flow away from the proximal sides. Concurrently, low compressive normal stress on the proximal sides of bumps allows the soil there to swell, causing pore fluid to be drawn toward the distal sides of bumps. As we have shown, the distribution of normal stress on the slip surface determines R. Energy is dissipated by means of the flow process during forced circulation. Sliding by the mechanism of forced circulation is rate dependent, because forced circulation is a diffusive and hence a rate-dependent process that depends on the hydraulic conductivity of the soil and the path length of diffusion.

Our model for forced circulation applies to landslides that fail in a ductile manner (without sudden loss of strength), such as landslides on natural slopes that fail by a gradual rise of the water table. Landslides having slip surfaces are very common and observations indicate that slip surfaces of landslides in clayey materials commonly are wavy (Mizuno, 1989, p. 96, 105). Thus, we believe our model applies to most landslides that have relatively steady motion. Driving forces in natural slopes tend to be near equilibrium with the residual strength of the soil (Skempton, 1964). Any strength that is lost in the failure of such slopes generally is lost progressively (Bjerrum, 1967; Palmer and Rice, 1973). However, in slopes that fail in a brittle manner (a sudden or abrupt loss of strength accompanies failure), such as rock slopes or slopes underlain by quick clay, driving forces are sufficient to overcome the peak strength of the material and roughness of the failure surface cannot retard sliding to a degree sufficient to prevent acceleration of the failed mass.

We have solved a boundary-value problem that models forced circulation as the deformation and fluid flow occurring in a porous elastic solid that is sliding over a wavy, impermeable, rigid surface (details of the solution follow in succeeding sections of this paper). Solving this problem

allowed us to determine the normal stress on the slip surface and thus compute a formula for R due to forced circulation,

$$R = -\bar{v}_x (Al)^2 \gamma_w \frac{(1-2\mu)^2}{4Kl(1-\mu)^2}. \quad (6)$$

In equation 6, $\bar{v}_x$ is the mean velocity of the landslide, parallel to x; γ_w is the unit weight of water, A is the amplitude of the bumps, K is the hydraulic conductivity of the landslide debris, l is the wave number, equal to $2\pi/L$; L is the wavelength of sinusoidal bumps on the slip surface; (Al), the product of the amplitude and the wave number, is the maximum local slope of the slip surface with respect to x;, and μ is Poisson's ratio for drained deformation of the soil. Hereafter, Al is called the roughness.

Equation 6 helps to explain how a landslide can maintain equilibrium even when shear strength at the basal slip surface decreases due to an increase in the average pore-water pressure at the basal slip surface. If equation 6 is substituted into equation 5c, the following is obtained:

$$\gamma_t Z \sin\alpha = \frac{1}{L}\int_0^L (c' - \{[T_{nn}]_{z_0} + [P]_{z_0}\}\tan\phi')\,dx + \bar{v}_x (Al)^2 \gamma_w \frac{(1-2\mu)^2}{4Kl(1-\mu)^2}. \quad (7)$$

According to equation 7, if the average shear strength of the slip surface (the integral on the right side of equation 7) decreases, due to a decrease in effective stress, the landslide can stay in equilibrium if R increases. Thus, R can increase if the velocity, $\bar{v}_x$, increases, because other parameters that determine R are nearly constant in a given landslide.

Our formula (equation 6) for resistance to sliding of a landslide, by the mechanism of forced circulation, is similar to the result Kamb (1970) obtained for a temperate glacier sliding on a wavy bedrock surface by a mechanism of rate-dependent plastic deformation (viscous flow). Kamb's (1970) formula for R, in our notation, is

$$R = -\bar{v}_x \eta (Al)^2 \frac{l}{2}, \quad (8a)$$

where η is the viscosity of glacier ice.

However, our equation 6 differs in basic form from the formula derived by Mizuno (1989) for resistance to sliding. Mizuno (1989) assumed that landslide debris slides over an uneven slip surface by the mechanism of soil creep. Creep is used in the sense of undrained plastic deformation of a triaxial specimen subject to a constant load that is a fraction of the static load needed to cause failure. Mizuno's (1989) formula for resistance to sliding (in our notation) is

$$R = -\frac{\pi(Al)}{4b}\ln\left(\frac{2(Al)\bar{v}_x}{\pi a}\right), \quad (8b)$$

where a and b are constants to be determined from field data, a has units of velocity, and b has units of inverse stress.

Mizuno's (1989) corresponding formula for predicting velocity of a landslide from R is

$$\bar{v}_x = \frac{a\pi}{2(Al)}\exp\left(\frac{-4bR}{\pi(Al)}\right). \quad (8c)$$

Note that Mizuno's (1989) formula indicates an exponential relationship between R and $\bar{v}_x$, whereas our formula (equation 6) indicates a linear relationship between R and $\bar{v}_x$.

PRELIMINARY ANALYSIS OF THE EFFECT OF FORCED CIRCULATION ON THE MOVEMENT OF LANDSLIDES

We model a landslide as a deformable body that slides at a constant velocity past a rigid body (fig. D9). The boundary (that is, interface) between the bodies undulates. It is assumed that variation of stresses generated by acceleration is negligible near the interface and that no cavitation occurs at the interface. The undulations are assumed to be wide, symmetrical, low-amplitude steps. Movement is assumed parallel to the x-axis, and the undulations are assumed to be periodic in x, and independent of y. Consequently, plane deformation is assumed to occur. The landslide is represented as an infinite strip bounded by $z=z_0$ and $z=z_1$, and moving parallel to the x-axis with a mean velocity of $\bar{v}_x$ (fig. D9). The basal slip surface, z_0, is a sinusoidal perturbation of the x-y plane:

$$z_0 = A\sin lx. \quad (9)$$

In order to investigate the resistance to sliding generated by forced circulation of pore water in a landslide, and the effect of that resistance on the velocity of the landslide, we assume that the landslide debris behaves like a fluid-infiltrated, porous-elastic solid (Biot, 1941; Rice and Cleary, 1976). We have chosen such a model for material behavior because the movement of pore water is considered the primary cause of time-dependent effects in fine-grained soils (Terzaghi, 1925; Wroth and Houlsby, 1985, p. 6).

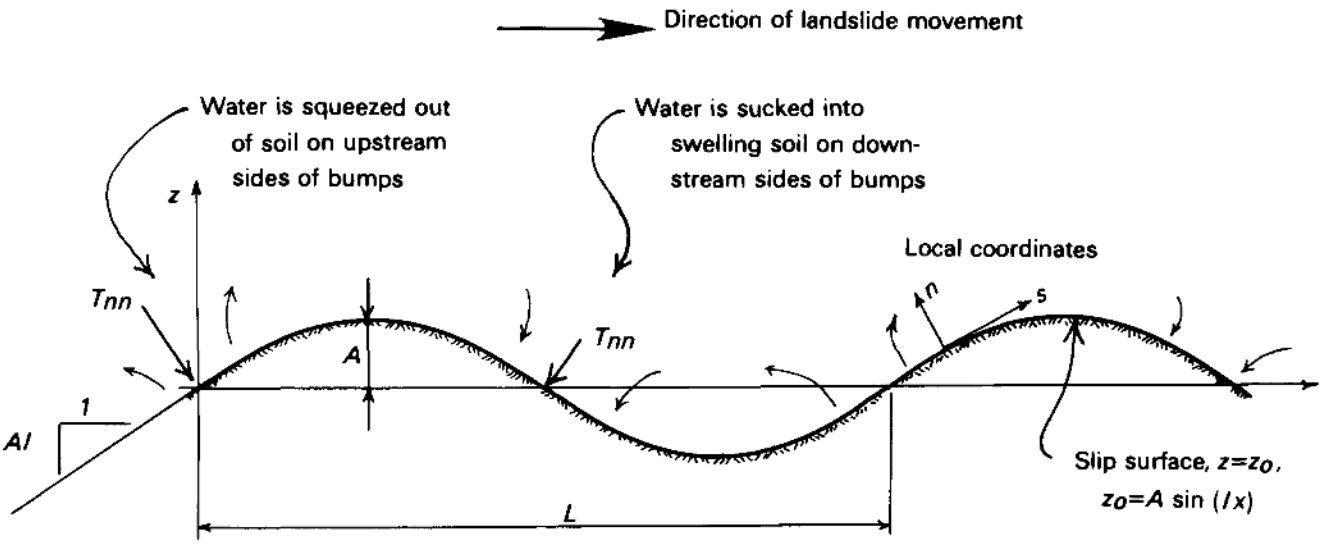

Figure D9. Features of the model used to analyze the resistance to sliding due to forced circulation. The ground surface is a plane, and the x- and z-axes are parallel and perpendicular to the ground surface, respectively. Sinusoidal undulations of the slip surface have wavelength L and amplitude A. The maximum local slope of the slip surface with respect to the x-axis is Al, where l is the wave number, $2\pi/L$. The landslide is moving toward the right so that the compressive stress, T_{nn} (shown by heavy arrows), is greater on the upstream sides of the bumps than on the downstream sides. The small curved arrows indicate that water is flowing away from the upstream sides of the bumps and is flowing toward the downstream sides of the bumps.

Perturbation Analysis of Equations Governing Stress and Pore-Water Movement

Stress and pore-water movement in the landslide are governed by the following equations:

$$\frac{\partial T_{xx}}{\partial x} + \frac{\partial T_{zx}}{\partial z} + \gamma_t \sin\alpha = 0 , \qquad (1a)$$

$$\frac{\partial T_{zx}}{\partial x} + \frac{\partial T_{zz}}{\partial z} - \gamma_t \cos\alpha = 0, \qquad (10a)$$

$$\nabla^2 \left(T_{xx} + T_{zz} + \frac{1-2\mu}{1-\mu} P \right) = 0, \qquad (10b)$$

and

$$\frac{2KG(1-\mu)}{\gamma_w (1-2\mu)} \nabla^2 (T_{xx} + T_{zz} + 2P) = \frac{\partial}{\partial t} (T_{xx} + T_{zz} + 2P) . \qquad (10c)$$

Equations 1a and 10a are the equilibrium equations, equation 10b is the compatibility equation for stress diffusion (Rice and Cleary, 1976), and equation 10c is the stress-diffusion equation (Rice and Cleary, 1976). In equations 10b and 10c, P is the pore-water pressure, K is the hydraulic conductivity, γ_w is the unit weight of water, G is the shear modulus, and μ is Poisson's ratio for drained deformation. We assume that the soil skeleton is incompressible, so the coefficients appearing in 10b and 10c are simpler than their counterparts in Rice and Cleary (1976).

We use perturbation expansions of the field variables to determine the stresses and pore pressure caused by deformation near the wavy slip surface. The expansions are in powers of Al, which is the maximum local slope of the slip surface (with respect to x); Al, is small compared to unity. Then $(Al)^2$ must be small compared to Al. The pressure, P, and the stress components; T_{xx}, T_{zx}, and T_{zz}; are determined by the following expansions:

$$P = \bar{P} + \tilde{P} + \mathbf{O}(Al)^2. \qquad (11a)$$

$$T_{xx} = \bar{T}_{xx} + \tilde{T}_{xx} + \mathbf{O}(Al)^2, \qquad (11b)$$

$$T_{zx} = \bar{T}_{zx} + \tilde{T}_{zx} + \mathbf{O}(Al)^2, \qquad (11c)$$

and

$$T_{zz} = \bar{T}_{zz} + \tilde{T}_{zz} + \mathbf{O}(Al)^2, \qquad (11d)$$

where $\mathbf{O}(Al)^2$ is the remainder term on the order of $(Al)^2$.

The zero-order components of the stresses are known from the infinite slope analysis and solutions for problems in elasticity (Lambe and Whitman, 1969, p. 353–356; Jaeger and Cook, 1969, p. 356),

$$\bar{T}_{zz} = \gamma_t (z - z_1) \cos\alpha, \tag{12a}$$

$$\bar{T}_{zx} = \gamma_t (z_1 - z) \sin\alpha, \tag{12b}$$

$$\bar{T}_{xx} = \frac{\mu}{(1-\mu)} \gamma_t (z - z_1) \cos\alpha. \tag{12c}$$

Likewise, the zero-order pore pressure for slope-parallel flow (we assume that the slip surface is impermeable) is determined by the following:

$$\bar{P} = (h - z)\gamma_w \cos\alpha; \quad z \le h. \tag{13a}$$

The pore pressure is part of the head, H, that drives groundwater flow. The complete expansion for the head is

$$\gamma_w H = \gamma_w (z \cos\alpha - x \sin\alpha + Y_0) + (h - z)\gamma_w (\cos\alpha) + \tilde{P} + \mathbf{O}(Al)^2; \quad z \le h. \tag{13b}$$

In equation 13b, Y_0 is the elevation of the origin of the x-z coordinate system above some arbitrary datum, and h is the height of the water table above the x axis.

We note that the zero-order stresses and pore pressure are independent of x and t. By substituting equations 11a, 11b, 11c, 11d, 12a, 12b, 12c, and 13a into equations 1a and 10a, 10b, and 10c, we derive the following for the first-order variables:

$$\frac{\partial \tilde{T}_{xx}}{\partial x} + \frac{\partial \tilde{T}_{xz}}{\partial z} = 0, \tag{14a}$$

$$\frac{\partial \tilde{T}_{zx}}{\partial x} + \frac{\partial \tilde{T}_{zz}}{\partial z} = 0, \tag{14b}$$

$$\nabla^2 (\tilde{T}_{xx} + \tilde{T}_{zz} + \frac{1 - 2\mu}{1 - \mu} \tilde{P}) = 0, \tag{14c}$$

and

$$\frac{2KG(1-\mu)}{\gamma_w (1-2\mu)} \nabla^2 (\tilde{T}_{xx} + \tilde{T}_{zz} + 2\tilde{P}) = \frac{\partial}{\partial t} (\tilde{T}_{xx} + \tilde{T}_{zz} + 2\tilde{P}). \tag{14d}$$

To simplify our analysis of the mechanism of forced circulation, we assume the landslide is moving at a steady rate, $\bar{v}_x$, and introduce a new system of coordinates that moves parallel with x in order to make the problem independent of time (Rosenthal, 1946). Only two independent variables, ξ and z, remain after transforming the coordinates. Let

$$\xi = x - \bar{v}_x t, \tag{15a}$$

and

$$\Theta = t. \tag{15b}$$

We use the chain rule for partial differentiation to obtain formulas for transforming partial derivatives to the ξ-z coordinate system,

$$\frac{\partial}{\partial x} = \left(\frac{\partial \xi}{\partial x}\right)\frac{\partial}{\partial \xi} + \left(\frac{\partial \Theta}{\partial x}\right)\frac{\partial}{\partial \Theta}, \tag{15c}$$

and

$$\frac{\partial}{\partial t} = \left(\frac{\partial \xi}{\partial t}\right)\frac{\partial}{\partial \xi} + \left(\frac{\partial \Theta}{\partial t}\right)\frac{\partial}{\partial \Theta}. \tag{15d}$$

The partial derivatives of ξ and Θ, appearing in equations 15c and 15d, are obtained by differentiating equations 15a and 15b with respect to x and t. The derivatives are $\partial\xi/\partial x=1$, $\partial\xi/\partial t=-\bar{v}_x$, $\partial\Theta/\partial x=0$, and $\partial\Theta/\partial t=1$. Note that $\partial/\partial\Theta=0$, because a steady state of deformation is observed in the new coordinate system. Equations 15c and 15d reduce to the following when the values of the derivatives are substituted into the equations:

$$\frac{\partial}{\partial x} = \frac{\partial}{\partial \xi}, \tag{15e}$$

and

$$\frac{\partial}{\partial t} = -\bar{v}_x \frac{\partial}{\partial \xi}. \tag{15f}$$

The field equation, 14d, for stress diffusion can be rewritten as

$$c\nabla^2(\tilde{T}_{xx}+\tilde{T}_{zz}+2\tilde{P}) = \frac{\partial}{\partial t}(\tilde{T}_{xx}+\tilde{T}_{zz}+2\tilde{P}), \quad (16a)$$

(Rice and Cleary, 1976, p. 230).

The diffusion constant, c, in equation 16a is determined by

$$c = \frac{2GK}{\gamma_w}\left(\frac{1-\mu}{1-2\mu}\right). \quad (16b)$$

where γ_w=9.8 kN/m^3 (Freeze and Cherry, 1979).

The field equation for stress diffusion in the new ξ-z coordinate system is

$$\nabla^2(\tilde{T}_{\xi\xi}+\tilde{T}_{zz}+2\tilde{P}) = \left(\frac{-\bar{v}_x}{c}\right)\partial\frac{(\tilde{T}_{\xi\xi}+\tilde{T}_{zz}+2\tilde{P})}{\partial\xi}. \quad (16c)$$

The term on the right side of equation 16c accounts for advection (conveyance) of water by the landslide debris.

If the absolute value of the coefficient, $\bar{v}_x/c$, is small compared to 1, then advection can be neglected (Kamb, 1970). For steady landslides in which $\bar{v}_x/K \leq 100$ and the debris has typical values for G and μ (G=10^7 Pa, μ=0.3; Lambe and Whitman, 1969), the coefficient on the right side of equation 16c is small compared to 1; $|-\bar{v}_x/c| \leq 0.03$. Advection causes a small phase shift in the solution for $(\tilde{T}_{\xi\xi}+\tilde{T}_{zz}+2\tilde{P})$ that has a negligible effect on the magnitude of $(\tilde{T}_{\xi\xi}+\tilde{T}_{zz}+2\tilde{P})$. Thus, Laplace's equation is a good approximation of the diffusion equation (16c):

$$\nabla^2(\tilde{T}_{\xi\xi}+\tilde{T}_{zz}+2\tilde{P}) = 0. \quad (16d)$$

Equation 16d, together with the compatibility equation, the equilibrium equations, the constitutive equations, and the boundary conditions govern the problem in the new coordinate system. Transformation of equations 14a, 14b, and 14c is accomplished by simply replacing the x's with ξ's.

Airy's stress function (Malvern, 1969) facilitates solution of equations 14a, 14b, 14c, and 16d. The stress function automatically satisfies the equilibrium equations; the following relationships hold between the stress components and the stress function:

$$\frac{\partial^2\tilde{\phi}}{\partial z^2} = \tilde{T}_{\xi\xi}, \quad (17a)$$

$$\frac{\partial^2\tilde{\phi}}{\partial\xi^2} = \tilde{T}_{zz}, \quad (17b)$$

and

$$\frac{\partial^2\tilde{\phi}}{\partial\xi\partial z} = -\tilde{T}_{z\xi}. \quad (17c)$$

When the stress function is substituted into the simplified diffusion equation (16d) and the compatibility equation (14c), two equations relating the stress function and the pore-pressure function are obtained,

$$\nabla^2[\nabla^2\tilde{\phi}+2\tilde{P}] = 0 \quad (18a)$$

and

$$\nabla^2\left[\nabla^2\tilde{\phi}+\left(\frac{1-2\mu}{1-\mu}\right)\tilde{P}\right] = 0. \quad (18b)$$

The Laplacian, ∇^2, is a linear operator and the quantities in square brackets in equations 18a and 18b satisfy Laplace's equation; therefore, any linear combination of these quantities also satisfy Laplace's equation. Equations 18a and 18b can be combined algebraically to show that $\tilde{P}$ satisfies Laplace's equation and $\tilde{\phi}$ satisfies the biharmonic equation:

$$\nabla^2\tilde{P} = 0 \quad (18c)$$

$$\nabla^4\tilde{\phi} = 0 \quad (18d)$$

Thus, we solve equations 18c and 18d subject to boundary conditions at the slip surface, in order to determine the relationship between the rate of movement and the resistance to sliding due to forced circulation.

Derivation of Boundary Conditions for Sliding and Forced Circulation

We have made several assumptions in setting up a boundary value problem that describes forced circulation of water as a landslide moves over its slip surface. Many of the assumptions are embodied in the boundary conditions.

A boundary condition on z_0 is that sliding is tangential to z_0,

$$[v_n]_{z_0} = 0. \quad (19a)$$

This assumption is consistent with our observations of slip surfaces and with the observations of others (for example, Lambe and Whitman, 1969) that soil subject to constant normal load shears at constant volume once the residual strength

is attained. This assumption (equation 19a) would be violated if our model included (Coulomb-type) plastic deformation, because dilation would occur at the slip surface (Savage and Smith, 1986)

The velocity, v_n, can be written in terms of the x and z components of velocity, v_x and v_z,

$$[v_n]_{z_0} = -[v_x]_{z_0} \sin\theta + [v_z]_{z_0} \cos\theta. \quad (19b)$$

In equation 19b, θ is the counterclockwise angle between the x-axis and a line tangent to z_0; thus,

$$\tan\theta = \frac{dz_0}{dx}. \quad (19c)$$

If we set v_n equal to zero in equation 19b and solve for v_z, we determine that

$$[v_z]_{z_0} = [v_x]_{z_0} \tan\theta. \quad (19d)$$

We can expand the components of the velocity in a perturbation series as we have done for the stresses,

$$v_x = \bar{v}_x + \tilde{v}_x + \mathbf{O}(Al)^2, \quad (20a)$$

and

$$v_z = \bar{v}_z + \tilde{v}_z + \mathbf{O}(Al)^2, \quad (20b)$$

but

$$\bar{v}_x = \text{constant}, \quad (20c)$$

and

$$\bar{v}_z = 0, \quad (20d)$$

where $\bar{v}_x$ is the constant rate of sliding in the absence of slip-surface irregularities; $\bar{v}_z$ is zero because sliding is assumed to be parallel to the x-axis.

When equations 19c, 20a, and 20b are substituted into equation 19d, a boundary condition for $\tilde{v}_z$ results:

$$[\bar{v}_z + \tilde{v}_z + \mathbf{O}(Al)^2]_{z_0} = [\bar{v}_x + \tilde{v}_x + \mathbf{O}(Al)^2]_{z_0} \frac{dz_0}{dx}.$$

We previously defined $\bar{v}_z$ and $\bar{v}_x$ to be constants, independent of x and z (equations 20c, 20d); $\bar{v}_z$ is zero because the average movement is parallel to the x-axis and the mean slope of the slip surface. The term $\tilde{v}_x(dz_0/dx)$ is second order because it is the product of two first order quantities, $\tilde{v}_x$ and (dz_0/dx). By dropping terms higher than first order, the relationship between $[v_x]_{z_0}$ and $[v_z]_{z_0}$ reduces to

$$[\tilde{v}_z]_{z_0} = \bar{v}_x \left(\frac{dz_0}{dx}\right). \quad (21)$$

Formulas similar to equation 21 have been used by Nye (1969), Kamb (1970), and Morland (1976a). The geometry of the slip surface enters the solution of equations 18c and 18d through equation 21.

A second boundary condition concerns the shear stress at the slip surface. The obvious assumption is that the shear stress is determined by the yield criterion (equation 5a). The normal stress $[T_{nn}]_{z_0}$, shear stress $[T_{ns}]_{z_0}$, and pore water pressure $[P]_{z_0}$, can be expanded (as in equations 11a, 11b, 11c, and 11d) in the yield criterion,

$$[\bar{T}_{ns} + \tilde{T}_{ns} + \mathbf{O}(Al)^2]_{z_0}$$

$$= c' - [\bar{T}_{nn} + \bar{P} + \tilde{T}_{nn} + \tilde{P} + \mathbf{O}(Al)^2]_{z_0} \tan\phi'. \quad (22a)$$

Equation 22a can be resolved into two equations by collecting terms of zero and first order and deleting terms of second order,

$$[\bar{T}_{ns}]_{z_0} = c' - [\bar{T}_{nn} + \bar{P}]_{z_0} \tan\phi', \quad (22b)$$

and

$$[\tilde{T}_{ns}]_{z_0} = -[\tilde{T}_{nn} + \tilde{P}]_{z_0} \tan\phi'. \quad (22c)$$

The zero-order shear stress is a constant. In the zero-order approximation, the slip surface is a plane parallel to the x-axis so $[\bar{T}_{ns}]_{z_0} = [\bar{T}_{zx}]_{z_0}$ and $[T_{nn}]_{z_0} = [T_{zz}]_{z_0}$. Thus, the zero-order shear stress is determined by substituting equations 13 and 17a into equation 22b,

$$[\bar{T}_{zx}]_{z_0} = c' + (Z\gamma_t - h\gamma_w)(\cos\alpha)(\tan\phi'). \quad (22d)$$

We have analyzed and attempted to solve a boundary-value problem that models forced circulation with Coulomb friction at the boundary (first-order shear stress determined by equation 22c). However, we were unable to determine an appropriate boundary condition to replace equations 19a or 21, because Coulomb friction at the boundary would cause dilation and contraction at the slip surface.

In order to overcome the difficulties connected with using equation 22c as a boundary condition, we have assumed that the first-order shear stress is zero everywhere on the boundary,

$$[\tilde{T}_{ns}]_{z_0} = 0. \tag{23}$$

This assumption is equivalent to letting the coefficient of friction in equation 22c be zero. The coefficient of residual friction of clayey materials ranges from 0.08 to 0.36 (Skempton, 1964; Lambe and Whitman, 1969). This assumption results in the constants being determined by a system of linear equations that are readily solved.

We use the standard equations for transformation of stress (Hill, 1950, p. 347) to put equation 23 in terms of $[\tilde{T}_{zx}]_{z_0}$,

$$\tilde{T}_{ns} \approx (\tilde{T}_{zz} - \tilde{T}_{xx}) \sin\theta \cos\theta + \tilde{T}_{zx}(\cos^2\theta - \sin^2\theta). \tag{24a}$$

Leading terms in the Taylor series expansions of cos θ, sin θ, and tan θ are 1, θ, and θ, respectively. If we neglect higher order terms in the Taylor expansions, we can write

$$\tilde{T}_{ns} \approx (\tilde{T}_{zz} - \tilde{T}_{xx})\theta + \tilde{T}_{zx}(1 - \theta^2). \tag{24b}$$

Recall that $\tan\theta = Al\cos(lx)$, and that for small θ, $\theta \approx \tan\theta$; thus $\theta \approx Al\cos(lx)$. Making this substitution of tan θ for θ shows that the right side of equation 24b consists of one first-order term, $\tilde{T}_{zx}$, and some second-order terms,

$$\tilde{T}_{ns} = \tilde{T}_{zx} + \mathbf{O}(Al)^2. \tag{24c}$$

Thus, we replace equation 23 with

$$[\tilde{T}_{zx}]_{z_0} = 0, \tag{25a}$$

or in the moving coordinate system,

$$[\tilde{T}_{z\xi}]_{z_0} = 0. \tag{25b}$$

The velocity of the landslide also enters the solution of equations 18c and 18d through the flow at the wavy boundary. We assume that the slip surface is impermeable to water, so that

$$[q_n]_{z_0} = 0, \tag{26}$$

In equation 26, q_n is the component of the specific discharge that is normal to the slip surface. We can rewrite equation 26 in terms of q_x and q_z by expanding them in terms of perturbation series,

$$q_x = \bar{q}_x + \tilde{q}_x + \mathbf{O}(Al)^2, \tag{27a}$$

and

$$q_z = \bar{q}_z + \tilde{q}_z + \mathbf{O}(Al)^2. \tag{27b}$$

By following steps similar to those used in deriving equation 21 from equation 19a, we determine that

$$[q_z]_{z_0} = \bar{q}_x\left(\frac{dz_0}{dx}\right). \tag{27c}$$

In equations 27a and 27b

$$\bar{q}_x = -K\tan\alpha, \text{ a constant}, \tag{27d}$$

and

$$\bar{q}_z = 0, \tag{27e}$$

because mean flow is assumed to be parallel to the slope. For landslides on gentle to moderate slopes ($\alpha \leq 15°$), $\tan\alpha = \mathbf{O}(Al)$. Thus, substituting equation 27d into 27c, shows that $[q_z]_{z_0} = \mathbf{O}(Al)^2$, so that it can be neglected in the continuity equation, thus

$$[\tilde{q}_z]_{z_0} = 0. \tag{27f}$$

To relate the components of flow to the volumetric strains at the slip surface, we use a form of the continuity equation derived by combining equations A2.9, A2.10, and A2.12 of Freeze and Cherry (1979, p. 532).

$$-\frac{\partial q_x}{\partial x} - \frac{\partial q_z}{\partial z} = n\beta\frac{DP}{Dt} + \frac{\partial v_x}{\partial x} + \frac{\partial v_z}{\partial z}. \tag{28}$$

In equation 28, β represents the compressibility of water, n represents the porosity of the soil, q_x and q_z are components of the specific discharge vector or Darcy velocity vector of the fluid relative to the grains, v_x and v_z are components of the velocity vector of the solid, and DP/Dt is the total-time or material-time derivative,

$$\frac{DP}{Dt} = v_x \frac{\partial P}{\partial x} + v_z \frac{\partial P}{\partial z} + \frac{\partial P}{\partial t} .$$

Equation 28 is a mathematical statement of the law of conservation of mass for the fluid and solids that constitute the landslide material. The equation ensures that the change in mass of fluid within a representative elemental volume of the material is balanced by flow of water and solids into or out of the element.

When equations 11a, 13a, 20a, 20b, 20c, 20d, and 27a, 27b, 27d, 27e, and 27f are substituted into equation 28 and terms of $\mathbf{O}(Al)^2$ are dropped, the expression becomes

$$\frac{-\partial \tilde{q}_x}{\partial x} = n\beta\left(\bar{v}_x \frac{\partial \tilde{P}}{\partial x} + \tilde{v}_z \frac{\partial \bar{P}}{\partial z} + \frac{\partial \tilde{P}}{\partial t}\right) + \frac{\partial \tilde{v}_x}{\partial x} + \frac{\partial \tilde{v}_z}{\partial z} , \quad (29)$$

because the x and t derivatives of the zero-order quantities $\bar{q}_x$, $\bar{q}_z$, $\bar{P}$, $\bar{v}_x$, and $\bar{v}_z$, are zero (the zero order quantities are all constants with respect to x and t.)

Let

$$\frac{\partial \tilde{v}_x}{\partial x} + \frac{\partial \tilde{v}_z}{\partial z} \approx \frac{\partial \tilde{e}}{\partial t} , \quad (30)$$

for small strains, where $\tilde{e}$ is the volumetric strain, and $\partial\tilde{e}/\partial t$ is the rate of volumetric strain. In equation 30,

$$\tilde{e} = \tilde{E}_{xx} + \tilde{E}_{zz}, \quad (31)$$

where $\tilde{E}_{xx}$ and $\tilde{E}_{zz}$ are the normal components of strain.

When equations 30, 15c, and 15f are combined with equation 29, it simplifies to

$$-\frac{\partial \tilde{q}_\xi}{\partial \xi} = n\beta \tilde{v}_z \frac{\partial \bar{P}}{\partial z} - \bar{v}_x \frac{\partial \tilde{e}}{\partial \xi} . \quad (32)$$

However, the quantity $n\beta$ is small compared to Al, so that the first term on the right side of equation 32 can be neglected in a first-order analysis.

The specific discharge, $\tilde{q}_\xi$, is determined by Darcy's law,

$$\tilde{q}_\xi = -\frac{K}{\gamma_w} \frac{\partial \tilde{P}}{\partial \xi} . \quad (33)$$

The elevation head does not appear in equation 33, because the elevation head is a zero-order quantity. We substitute equation 33 into equation 32 and neglect the first term on the right side to derive

$$\left[\frac{\partial^2 \tilde{P}}{\partial \xi^2}\right]_{z_0} = -\left(\frac{\bar{v}_x \gamma_w}{K}\right)\left[\frac{\partial \tilde{e}}{\partial \xi}\right]_{z_0} . \quad (34)$$

Equation 34 relates fluid flow to volume change at the slip surface. Equations 21, 25b, and 34 determine the boundary conditions needed to solve the boundary-value problem that models forced circulation.

Solution for the Stresses and Velocities in the Porous-Elastic Material

We use the first-order approximations of the boundary conditions (equations 21, 25b, and 34) to guess the form of the pore-pressure function, $\tilde{P}$, which satisfies equation 18c and the stress function, $\tilde{\phi}$, which satisfies equation 18d,

$$\tilde{P} = \exp(-lz)\,[c_1 \cos\, l\xi + c_2 \sin\, l\xi] \quad (35a)$$

and

$$\tilde{\phi} = (c_3 + c_4 lz)\exp(-lz)\,[c_5 \cos\, l\xi + c_6 \sin\, l\xi] . \quad (35b)$$

Note that equation 35b is an incomplete solution of equation 18d. In a complete solution, $\exp(-lz)$ would be replaced by $[\exp(-lz)+c_7 \exp(lz)]$. We can neglect the $\exp(lz)$ part of the solution because the effects of forced circulation are greatest near the slip surface and we expect them to be undetectable at heights above the slip surface where z is greater than L.

We proceed to solve equations 35a and 35b together with the boundary conditions for the velocities, stresses, and the pore pressure. Then we compute the resistance to sliding from the solution for the normal stress, $T_{\xi\xi}$.

The free-slip boundary condition (equation 25) in terms of $\tilde{\phi}$ and the quasi-static coordinate system is,

$$\left[\frac{\partial^2 \tilde{\phi}}{\partial \xi \partial z}\right]_{z_0} = 0 , \quad (36)$$

where $\partial^2\tilde{\phi}/\partial\xi\partial z$ is determined by

$$\frac{\partial^2 \tilde{\phi}}{\partial \xi \partial z} = -l^2\,[c_3 + c_4 (lz - 1)]\exp(-lz)$$

$$(-c_5 \sin\, l\xi + c_6 \cos\, l\xi). \quad (37)$$

When equation 36 is substituted into equation 37, and z is set equal to zero, we determine that

$$c_3 = c_4 \tag{38}$$

Thus, c_3 and c_4 can be set equal to unity and their numerical value can be absorbed into c_5 and c_6.

To apply the velocity boundary condition, equation 21, we use the definition of v_z and transform coordinates; thus,

$$\tilde{v}_z = \left(\frac{\partial \tilde{u}_z}{\partial t}\right) \rightarrow \tilde{v}_z = -\bar{v}_x \left(\frac{\partial \tilde{u}_z}{\partial \xi}\right)$$

We compute $\tilde{u}_z$ by integrating the constitutive equation relating $\tilde{T}_{zz}$ and $\tilde{E}_{zz}$.

The constitutive equations that govern the behavior of the porous-elastic solid are listed in Rice and Cleary (1976). We have assumed that the soil particles are incompressible, so that the pore-pressure coefficient, B (Skempton, 1954; Lambe and Whitman, 1969), is equal to one, and Poisson's ratio for undrained loading, μ_u, is 0.5. For this assumption, the constitutive equations of Rice and Cleary (1976, p. 229) simplify to the following equations (in terms of the new coordinate system, equations 31):

$$2G\tilde{E}_{\xi\xi} = \tilde{T}_{\xi\xi} - \mu\,(\tilde{T}_{\xi\xi} + \tilde{T}_{zz}) + (1-2\mu)\,\tilde{P}, \tag{39a}$$

$$2G\tilde{E}_{z\xi} = \tilde{T}_{z\xi}, \tag{39b}$$

and

$$2G\tilde{E}_{zz} = \tilde{T}_{zz} - \mu\,(\tilde{T}_{\xi\xi} + \tilde{T}_{zz}) + (1-2\mu)\,\tilde{P}. \tag{39c}$$

After making the appropriate substitutions for the stress function into equation 39c, we integrate to derive an expression for $\tilde{v}_z$:

$$\tilde{v}_z = \left(\frac{-\bar{v}_x}{2G}\right)\frac{\partial}{\partial \xi}\int\left\{\frac{\partial^2\tilde{\phi}}{\partial \xi^2} - \mu\nabla^2\tilde{\phi} + (1-2\mu)\,\tilde{P}\right\}dz + f(\xi). \tag{40}$$

In equation 40, $f(\xi)$ must be zero, because $\tilde{v}_z \rightarrow 0$ as $z \rightarrow \infty$. We perform the operations indicated in equation 40 to obtain an expression for $\tilde{v}_z$,

$$\tilde{v}_z = \frac{-\bar{v}_x}{2G}\exp(-lz)\,\{-l\,[l\,(2+lz)\,c_5 - 2l\mu c_5 - (1-2\mu)\,\frac{c_1}{l}]\sin l\xi + l\,[l\,(2+lz)\,c_6 - 2l\mu c_6 - (1-2\mu)\,\frac{c_2}{l}]\cos\ l\xi\,\}. \tag{41}$$

In equation 41, z is set equal to zero, and the velocity boundary condition (equation 21) is used to solve for the constants; thus, by collecting sine and cosine terms, two expressions relating the constants are obtained

$$0 = 2lc_5 - 2l\mu c_5 - (1-2\mu)\,\frac{c_1}{l}, \tag{42a}$$

and

$$\bar{v}_x Al = \frac{-\bar{v}_x l}{2G}\left[2lc_6 - 2l\mu c_6 - (1-2\mu)\,\frac{c_2}{l}\right]. \tag{42b}$$

Equations 42a and 42b simplify to

$$c_1 = 2l^2\frac{(1-\mu)\,c_5}{1-2\mu} \tag{43a}$$

and

$$c_2 = \frac{2GAl + 2l^2\,(1-\mu)\,c_6}{1-2\mu} \tag{43b}$$

Now we use the boundary condition given by equation 34 to solve for c_5 and c_6. To compute $\tilde{e}$, we use equations 39a and 39c, and the definition of $\tilde{e}$:

$$\tilde{e} = \tilde{E}_{\xi\xi} + \tilde{E}_{zz}$$

Thus,

$$\tilde{e} = \frac{1-2\mu}{2G}\,\{\nabla^2\tilde{\phi} + 2\tilde{P}\}, \tag{44}$$

and

$$\frac{\partial \tilde{e}}{\partial \xi} = \frac{1-2\mu}{2G}\,\{-2l^3\exp(-lz)\,[-c_5\sin\ l\xi + c_6\cos\ l\xi] + 2l\,\exp(-lz)\,[-c_1\sin\ l\xi + c_2\cos\ l\xi]\}. \tag{45}$$

We differentiate equation 35a to compute an expression for $(\partial^2\tilde{P}/\partial\xi^2)$:

$$\frac{\partial^2 P}{\partial \xi^2} = -l^2 \exp(-lz)\{c_1 \cos l\xi + c_2 \sin l\xi\} . \quad (46)$$

Equations 45 and 46 are substituted into equation 34, the no-flow condition at the boundary, to obtain two more equations relating the unknown constants. When z is set equal to zero and the sine and cosine terms are collected, the following expressions are obtained.

$$lc_1 = \frac{\bar{v}_x \gamma_w (1-2\mu)}{KG}[-l^2 c_6 + c_2] \quad (47)$$

$$lc_2 = \frac{\bar{v}_x \gamma_w (1-2\mu)}{KG}[l^2 c_5 - c_1] . \quad (48)$$

Equations 43a, 43b, 47, and 48 constitute a system of four algebraic equations that can be solved simultaneously for the unknown constants, c_1, c_2, c_5, and c_6.

Resistance to Sliding Due to Forced Circulation

We can now compute the resistance to sliding due to forced circulation, using equations 4c, 12b, 17a, and 35b. Resistance to sliding due to roughness results only from the first order normal stress. The resistance to sliding due to the zero-order normal stress is zero, because (dz_0/dx) is periodic, $[\bar{T}_{xx}]_{z_0}$ is a constant, and the average value of (dz_0/dx) is zero,

$$0 = \frac{1}{L}\int_0^L [\bar{T}_{xx}]_{z_0}\left(\frac{dz_0}{dx}\right)dx. \quad (49a)$$

Thus, the resistance to sliding, R, is determined by substituting equations 31 into equation 4c

$$R = \frac{1}{L}\int_0^L [\tilde{T}_{\xi\xi}]_{z_0}\left(\frac{dz_0}{d\xi}\right)d\xi. \quad (49b)$$

On the boundary, the normal stress, $[T_{xx}]_{z_0}$, due to forced circulation is determined by substituting equations 35b and 38 into 17a,

$$[\tilde{T}_{\xi\xi}]_{z_0} = -l^2[c_5 \cos l\xi + c_6 \sin l\xi] . \quad (49c)$$

Equations 49c and 9 are substituted into equation 49b to compute R,

$$R = -\left(\frac{Al^3 c_5}{2}\right), \quad (50)$$

The constant c_5 is determined by solving equations 43a, 43b, 47 and 48 simultaneously:

$$c_5 = \frac{\bar{v}_x A \gamma_w (1-2\mu)^2}{2Kl^2(1-\mu)^2\left[1+\left(\frac{\bar{v}_x \gamma_w (1-2\mu)}{2KGl(1-\mu)}\right)^2\right]} . \quad (51)$$

The formula for R can now be written out fully by substituting equation 51 into 50:.

$$R = \frac{-\bar{v}_x (Al)^2 \gamma_w (1-2\mu)^2}{4Kl(1-\mu)^2\left[1+\left(\frac{\bar{v}_x \gamma_w (1-2\mu)}{2KGl(1-\mu)}\right)^2\right]} . \quad (52)$$

An approximate formula for R that applies when $\bar{v}_x/K \leq 100$ is derived by neglecting part of equation 52.

For combinations of $\bar{v}_x$, μ, G, and K typical for silty and clayey soils, the term $\left(\frac{\bar{v}_x \gamma_w (1-2\mu)}{2KGl(1-\mu)}\right)^2$ (in the denominator of equation 52) is small compared to 1. The resistance, R, is approximately

$$R \approx \frac{-\bar{v}_x (Al)^2 \gamma_w (1-2\mu)^2}{4Kl(1-\mu)^2} . \quad (53)$$

The corresponding expression for resistance to sliding due to plastic deformation at the base of a glacier (Kamb, 1970) is

$$R = -\frac{1}{2}\bar{v}_x (Al)^2 l\eta. \quad (54)$$

In equation 54, η is the viscosity of glacier ice. The negative sign in the right hand side of equations 50, 51, 52, 53, and 54 are a result of the sign convention used in computing the stresses. When R is substituted into equation 4b, it is clear that the resistance to sliding due to forced circulation augments the shear strength of the slip surface, because the negative sign preceding R in equation 4b cancels the negative sign in the formula for R.

For short wavelengths, the resistance due to forced circulation is small, and it increases with increasing wavelength, so that forced circulation will occur at short (perhaps

less than 10 m) wavelength bumps on the slip surface. This result is consistent with the fact that diffusion becomes more difficult as the path length, which is proportional to the wavelength, increases. At sufficiently long wavelengths, the resistance to sliding caused by forced circulation might become so great that some other mechanism of deformation becomes active near the slip surface, in much the same way that regelation gives way to viscous drag as the wavelength increases (Kamb, 1970). In glaciers, viscous drag is active at long wavelengths, because the viscous drag decreases with increasing wavelength (at constant roughness, equation 55). We do not know what mechanism in landslides might correspond to viscous drag in glaciers. One possibility is the creep deformation analyzed by Mizuno (1989); however, it appears to be independent of wavelength.

Equations 52 and 54 were derived for the case where the boundary is impermeable. If the boundary is permeable, pore-fluid diffusion is active at asperities having longer wavelengths (other things being equal), because the water flows through material beneath the landslide as well as through the slide, effectively reducing the resistance to flow of water. A permeable boundary has the same effect on the resistance to sliding, or the velocity of the landslide, as does increasing the permeability of the soil above the slip surface.

DISCUSSION AND CONCLUSION

Roughness of slip surfaces can affect the velocity of landslides. We have shown that forced circulation of water around asperities can control the velocity of a landslide.

We have not observed forced circulation occurring in landslides, but forced circulation is a plausible mechanism for the slow movement of landslides in clayey soils because most rate-dependent properties of soils have been attributed to the movement of pore water, and landslides move by sliding on uneven slip surfaces. Consolidation is considered the primary cause of time-dependent effects in fine-grained soils (Terzaghi, 1925; Wroth and Houlsby, 1985, p. 6). This suggests that movement of pore water might play an important role in controlling the velocities of landslides.

The mechanism of forced circulation is consistent with the observed linear relationship between landslide velocity and the average height of the water table (Terzaghi, 1950). In a wide, thin landslide where the water table is unconfined and flow is parallel to the ground surface, R is proportional to the mean pressure head at the slip surface, $h \cos \alpha$. The velocity dependent resistance to sliding, R, needed to maintain equilibrium is determined by the difference between the shear stress due to weight of the debris and the shear strength at the slip surface. An expression for R is determined by substituting equations 4c, 22d, and 49b into 4b and rearranging:

$$R = Z\gamma_t \left\{ \sin\alpha - \left[1 - \left(\frac{h\gamma_w}{Z\gamma_t} \right) \right] (\cos\alpha)\ (\tan\phi') \right\} - c' . \tag{55}$$

Equation 55 indicates that as the average pore pressure ($h\gamma_w$) at the slip surface rises, the shear strength due to friction on the slip surface decreases in proportion to the change in h, but the driving forces remain constant. Consequently, R must increase linearly as h increases, in order to provide enough resistance at the slip surface to compensate for the loss of shear strength and balance the driving forces acting on the landslide. This increase in R causes a corresponding increase in the velocity of the landslide.

For the mechanism of forced circulation, the velocity of the landslide, $\bar{v}_x$, is proportional to R. Rearranging equation 53 yields

$$\bar{v}_x = \frac{4KRl(1-\mu)^2}{(Al)^2\gamma_w(1-2\mu)^2}. \tag{56}$$

In equation 56, R is determined by equation 55. Thus, according to the mechanism of forced circulation (equations 55 and 56), the steady velocity increases linearly with the mean height of the water table. Furthermore, equations 55 and 56 indicate that the maximum velocity of a given landslide is determined by the maximum height attained by the average pressure head at the slip surface.

The relationship between velocity, shear stress, available shear strength, and resistance to sliding due to forced circulation are shown in figure D10. The shear stress tending to cause sliding is approximately constant, as indicated by the horizontal line in figure D10 (assuming that the total unit weight of soil does not change significantly through time). Sliding occurs when the water table exceeds its critical height, h_{cr}. When the critical height is exceeded, the shear stress exceeds the available shear strength, and sliding begins. However, the resistance to sliding due to forced circulation, R, augments the shear strength to exactly balance the shear stress and maintain equilibrium. If the average water table reaches some steady height, $\bar{h}$ (fig. D10), the slide will reach a steady velocity, $\bar{v}_x$, consistent with R.

The amount of resistance to sliding that can result from forced circulation is shown in figure D11. Figure D11*A* shows R graphed as a function of $\bar{v}_x/K$ for typical values of L, Al, μ, and γ_w. The graph shows R only for values of $\bar{v}_x/K \leq 100$ because we have neglected advective transport of water in deriving equation 54. Errors in R, due to neglecting advection, should become significant when $\bar{v}_x/K$ is greater than a few hundred. Figure D11*A* indicates that R is less than 5 kPa if $\bar{v}_x/K \leq 100$.

We expect the steady velocities of landslides in clayey soils to be correlated with the average hydraulic conductivity of the landslide material. Figure D11B shows $R/Z\gamma_t \sin\alpha$ (where $Z\gamma_t \sin\alpha$ is the shearing stress due to the weight of the

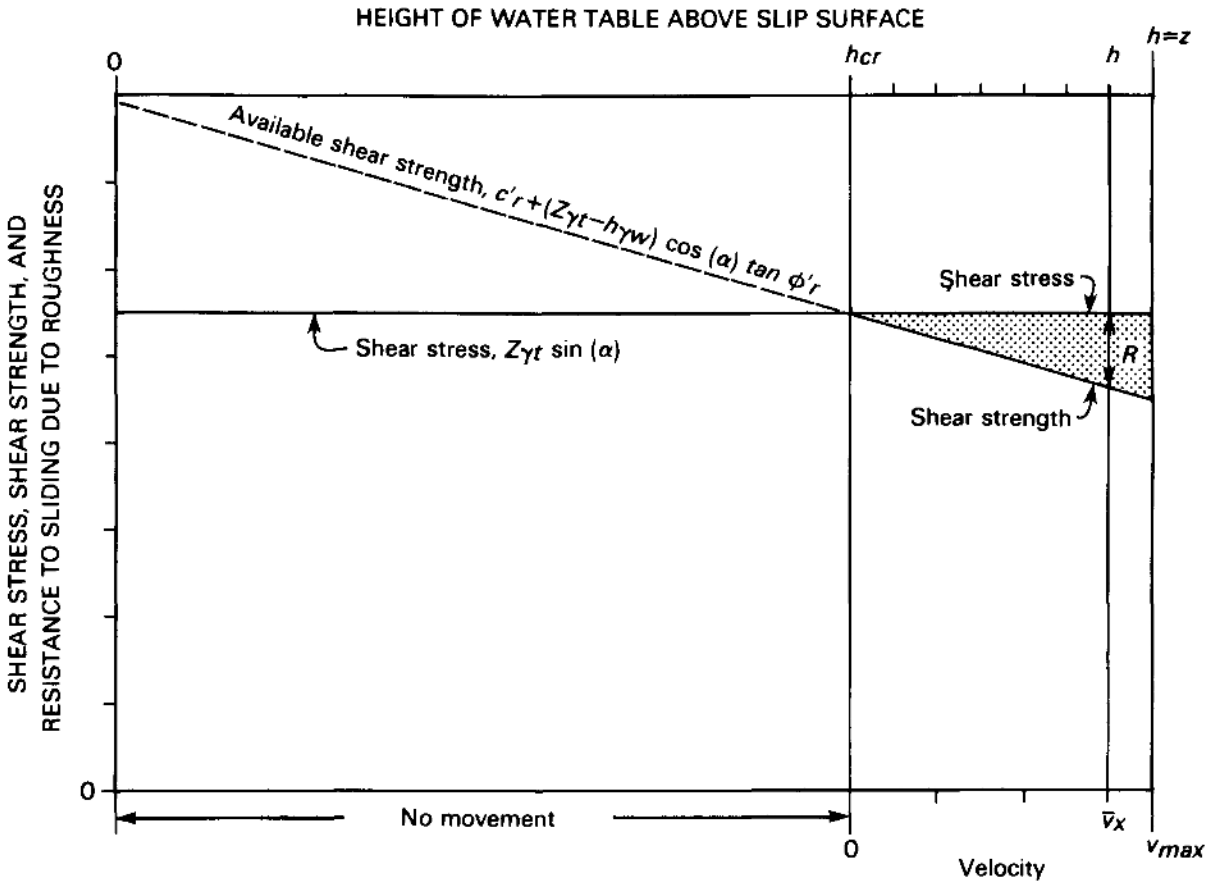

Figure D10. Relationship between shear strength, shear stress, the resistance to sliding due to roughness (R), mean height of water table above the slip surface (h), and the velocity of a landslide ($\bar{v}_x$). No movement occurs when $h \leq h_{cr}$, because the available shear strength exceeds the average shear stress. Movement occurs at velocity v_x when the water table is at a height, h, between the critical height and the maximum height ($h_{cr} \leq h \leq Z$), so that R plus the shear strength equals the average shear stress. The height of the shaded triangular area along any vertical line h – $\bar{v}_x$ is R.

landslide material) graphed as a function of $\bar{v}_x/K$. Of course, R must be less than or equal to the shear stress, $Z\gamma_t \sin \alpha$, and we expect it to be less than 10 percent of the shear stress in most cases. Figure D11*B* indicates that the maximum steady velocities of landslides should range from about one tenth to a few thousand times the hydraulic conductivity, assuming that $R/Z\gamma_t \sin \alpha$ rarely exceeds 0.1. Thus, a scatter plot of velocity versus hydraulic conductivity for various landslides should show a trend of landslides with higher hydraulic conductivity having greater velocities than those with lower conductivity.

The large range of velocities of steady landslides might be explained by the mechanism of forced circulation. The velocity of the landslide is proportional to the hydraulic conductivity, K, of the soil (equation 50). The conductivity of fine-grained soils ranges over several orders of magnitude, from 10^{-12} to 10^{-5} m/s (Freeze and Cherry, 1979, p. 29). The average velocities of steadily moving landslides in fine-grained soils also range over several orders of magnitude, from 10^{-10} to 10^{-3} m/s (Keefer and Johnson, 1983). A few landslides in clayey soils may actually move much faster than 10^{-3} m/s (R.M. Iverson, USGS, written commun., 1988). However, observations indicate that most landslides in clay soils, which have very low permeability, move steadily and slowly. For example, debris of the Aspen Grove landslide, near Ephraim, Utah, was clay and silty clay that presumably had a low permeability. The peak velocity of the landslide (Baum, 1988), which occurred when the water table was at the ground surface, was only 20 cm/day (2.3×10^{-6} m/s). The peak velocity of the Thistle landslide (Duncan and others, 1986, p. 11) was 48 m/day (5.6×10^{-4} m/s). Of landslides in clayey soils that were active in central Utah during 1983 and 1984, the Thistle landslide moved faster than any others we know of and the Aspen Grove landslide moved at a speed we consider typical of the landslides in central Utah.

Forced circulation will produce a complicated pattern of seepage within a moving landslide. For example, figure

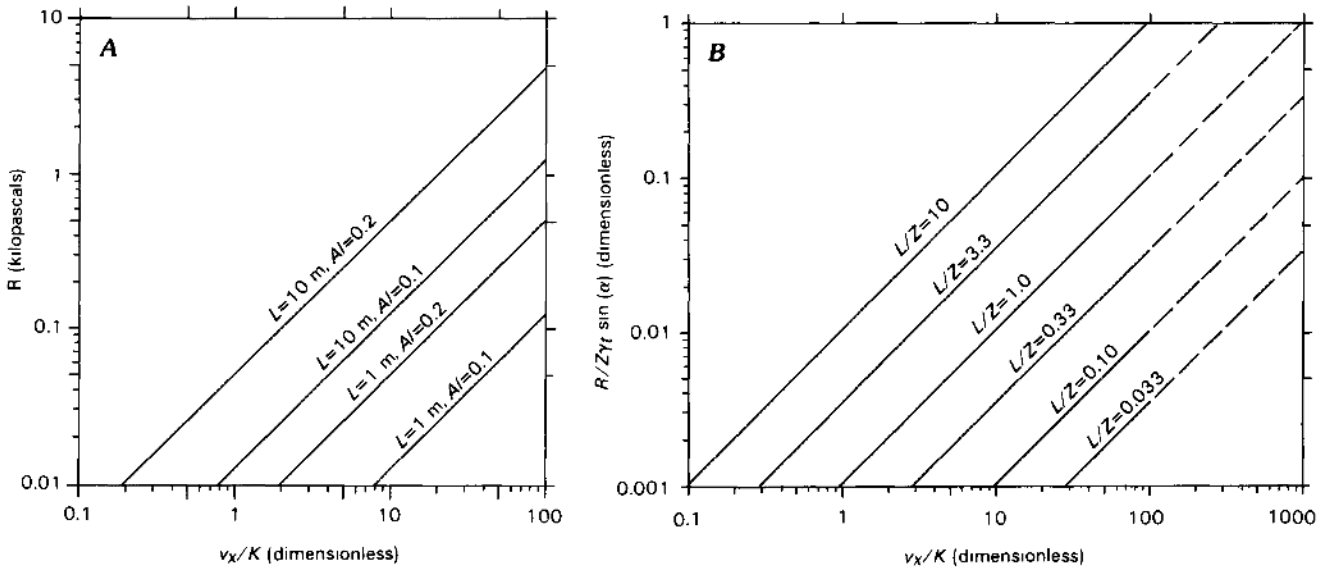

Figure D11. Graphs showing resistance to sliding due to forced circulation, R (computed using equation 53). (*A*) R is plotted against $\bar{v}_x/K$ for typical field values of the parameters; μ=0.3, γ_w=9.80 kN/m^3 (Lambe and Whitman, 1969); values of Al and L indicated on the graph are from Mizuno (1989). (*B*) R divided by the shear stress, $Z\gamma_t \sin \alpha$, is plotted against $\bar{v}_x/K$ for typical field values of the parameters: Z ranges from 1 to 30 m, γ_t=18.8 kN/m^3, γ_w=9.8 kN/m^3, μ=0.3 (Lambe and Whitman, 1969), α=15°, Al=0.2, and L ranges from 1 to 10 m.

D12 shows contours of total head in a landslide in which flow, due to forced circulation, is superposed on flow parallel to the slope with the water table at the ground surface. Total head, H, in figure D12, is determined by the formula,

$$H = z_1 \cos \alpha - x \sin \alpha + \frac{\bar{v}_x A}{K} \exp(-lz) \cos lx, \quad (57)$$

which is derived by substituting equation 35a into equation 13b. In equation 57, H is the head, z_1 is the height of the water table (and the ground surface) above the x-axis, α is the slope of the ground surface, and $\bar{v}_x A/K$ is the constant c_1 (equation 35a) divided by the unit weight of water, γ_w, for the case where μ is zero. The following parameters were used in equation 57 to determine the contours of head shown in figure D12: v_x/K is unity, l is 1 m^{-1}, A is 0.1 m, and z_1 is 2 m. For this combination of parameters, c_2 in equation 35a is approximately 0.0005 c_1, and, therefore, is negligible.

Although the details of the flow pattern resulting from forced circulation vary with the choice of parameters, some general features are illustrated by figure D12. Upward-directed flow, emanating from the proximal sides of the sinusoidal bumps, fans outward and some of the water seeps out of the ground surface along roughly horizontal flow lines (flow lines are perpendicular to contours of head). A small amount of water, emanating from the proximal side of a bump, flows upslope toward the zone of suction and dilation at the distal side of the neighboring bump. However, flow directed upslope might not occur in all cases. Flow near the distal sides of bumps is directed downward, and some water infiltrates from the ground surface in these areas.

The water level in observation wells (open tubes), or the pore pressure measured by piezometers, will depend on the position of the instrument with respect to the slip surface. The pore pressure near the distal sides of bumps ought to be lower than average, whereas the pore pressure near proximal sides of the bumps ought to be higher than average. However, testing the hypothesis of forced circulation by measuring pore pressure in an active landslide might have ambiguous results, because one needs to know the shape of the failure surface and the general pattern of groundwater flow in the slope in order to interpret the measurements.

We do not have enough field data to verify the mechanism of forced circulation, but at the Minor Creek landslide in northern California, the hydraulic conductivity is known well enough to use equation 53 to estimate the velocity. This landslide has an average hydraulic conductivity, K, of 5×10^{-8} m/s (Iverson and Major, 1987) and a maximum velocity of a few decimeters per month (Iverson, 1986), or from about 4×10^{-8} to 2×10^{-7} m/s. Using data from a stability analysis by Iverson and Major (1987), we calculate that R equals 0.13 kPa when the landslide is moving at its maximum velocity. Using this value for R and assuming that the wavelength, L, is between 1 and 10 m (range of wavelengths reported by Mizuno, 1989); the roughness, Al, is 0.2 (the average field value determined by Mizuno, 1989), and μ is 0.3; we calculate a maximum velocity for the Minor Creek landslide of 1.3×10^{-7} m/s (for L=1 m) or 1.3×10^{-8} m/s (for L=10 m). Our calculated velocities are of the same order of

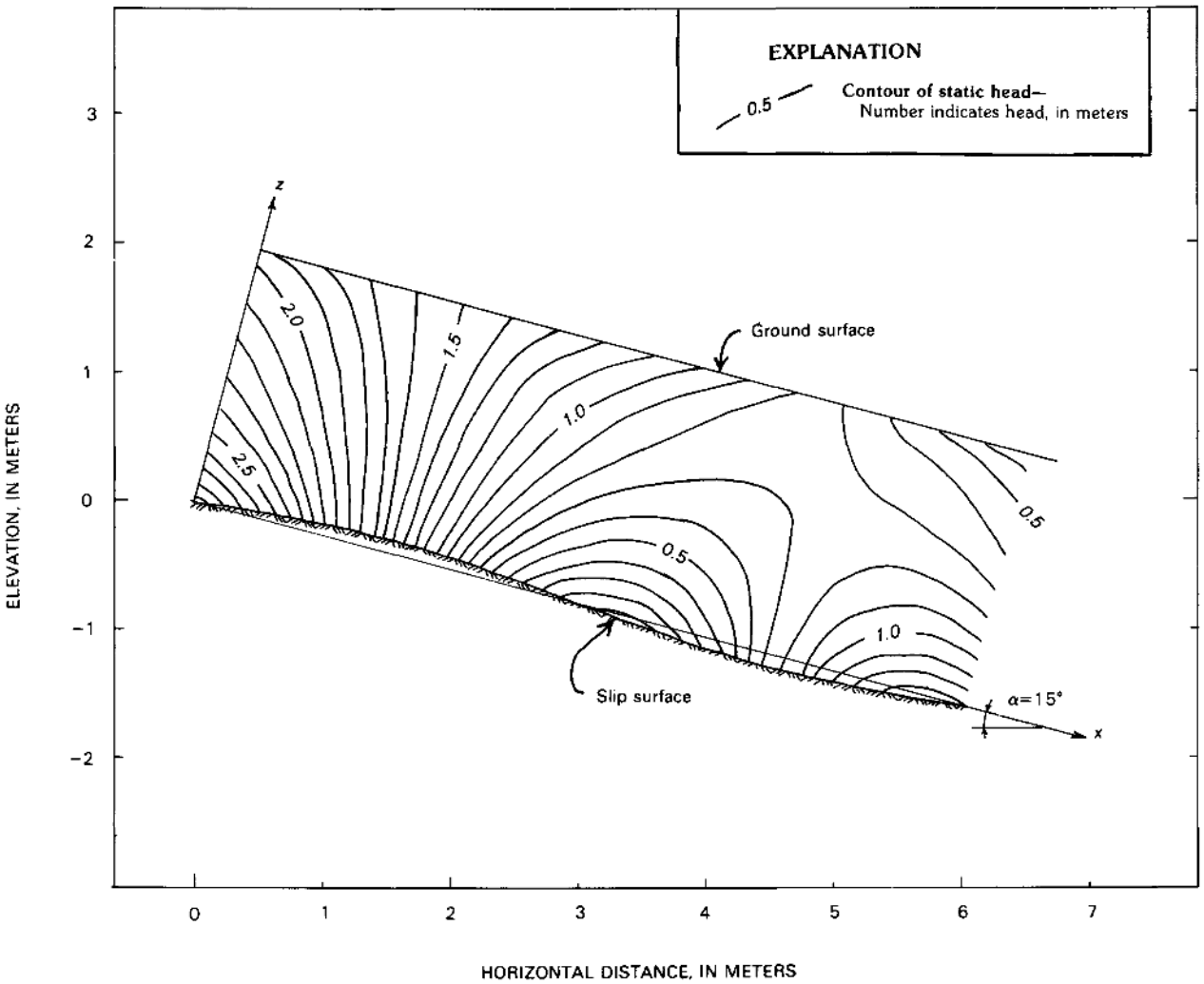

Figure D12. Cross section showing contours of total head, *H*, in a hypothetical landslide. The pattern of head results from the superposition of slope-parallel flow and forced circulation due to sliding on the uneven slip surface.

magnitude as the maximum velocity observed by Iverson (1986).

We expect our analysis of the mechanism of forced circulation to poorly represent operation of the mechanism in landslides that have been displaced less than one wavelength, and to represent the operation of forced circulation with acceptable accuracy in landslides that have been displaced at least a few wavelengths. Nonlinear deformation of soil, such as irreversible deformation that results in hysteresis during repeated cycles of loading and unloading, was not considered in our analysis. However, permanent deformation is greatest during the first cycle of loading and unloading, which would correspond to displacement of the landslide over one wavelength. Hysteresis diminishes during repeated cycles of loading and unloading of clay samples, or in other words, loading and unloading curves tend toward each other (Lambe and Whitman, 1969, p. 321) so that the modulus for unloading (swell index) approximately equals the modulus for loading (compression index). Thus, after a landslide has been displaced several wavelengths, hysteresis should be negligible, and equation 53 should determine the resistance due to forced circulation with fair accuracy.

REFERENCES CITED

Baum, R.L., 1988, The Aspen Grove landslide, Ephraim Canyon, central Utah: Cincinnati, Ohio, University of Cincinnati, Ph.D. thesis, 363 p.

Biot, M.A., 1941, General theory of three-dimensional consolidation: Journal of Applied Physics, v. 12, p. 155–164.

Bjerrum, Laurits, 1967, Progressive failure in slopes of over-consolidated plastic clay and clay shales: Journal of the Soil Mechanics and Foundations Division of the American Society of Civil Engineers, v. 93, no. SM5, p. 3–49.

Brunsden, Denys, 1984, Mudslides, *in* Brunsden, Denys, and Prior, D.B., eds., Slope instability: New York, Wiley, p. 363–418.

Budd, W.F., 1970a, Ice flow over bedrock perturbations: Journal of Glaciology, v. 9, no. 55, p. 29–48.

_____1970b, The longitudinal stress and strain-rate gradients in ice masses: Journal of Glaciology, v. 7, no 55., p. 19–27.

Byerlee, J.D., 1970, The mechanics of stick-slip: Tectonophysics, v. 19, no. 5, p. 475–486.

Collin, Alexandre, 1846, Recherches expérimentales sur les glissements spontanés des terrains argileux: Paris, Corps Royal des Ponts et Chausées *and* Corps des Mines. *Translation by* W.R. Schriever, 1956, Landslides in clays: Toronto, University of Toronto Press, 160 p.

Collins, I.F., 1968, On the use of the equilibrium equations and flow law in relating the surface and bed topography of glaciers and ice sheets: Journal of Glaciology, v. 7, no. 50, p. 199–204.

Craig, D., 1981, Mudslide plug flow within channels: Engineering Geology, v. 17, p. 273–281.

Dounias, G.T., Potts, D.M., and Vaughn, P.R., 1988, The shear strength of soils containing undulating shear zones—A numerical study: Canadian Geotechnical Journal, v. 25, p. 550–558.

Duncan, J.M., Fleming, R.W., and Patton, F.D., 1986, Report of the Thistle Slide Committee to State of Utah, Department of Natural Resources, Division of Water Rights: U.S. Geological Survey Open-File Report 86–505, 95 p.

Freeze, R.A., and Cherry, J.A., 1979, Groundwater: Englewood Cliffs, N.J., Prentice-Hall, 604 p.

Gould, J.P., 1960, A study of shear failure of certain Tertiary marine sediments, *in* Research conference on shear strength of cohesive soils, Boulder, Colorado: New York, American Society of Civil Engineers, p. 615–641.

Hill, Rodney, 1950, The mathematical theory of plasticity: Oxford, Clarendon Press, 356 p.

Hutchinson, J.N., 1970, A coastal mudflow on the London clay cliffs at Beltinge, North Kent [England]: Géotechnique, v. 20, no. 4, p. 412–438.

_____1983, Methods of locating slip surfaces in landslides: Bulletin of the Association of Engineering Geologists, v. 20, no. 3, p. 235–252.

Iverson, R.M., 1986, Dynamics of slow landslides—A theory for time-dependent behavior, *in* Abrahams, A.D., ed., Hillslope processes: Winchester, Mass., Allen & Unwin, p. 297–317.

Iverson, R.M., and Major, J.J., 1987, Rainfall, groundwater flow, and seasonal movement at Minor Creek landslide, northwestern California—Physical interpretation of empirical relations: Geological Society of America Bulletin, v. 99, p. 579–594.

Jaeger, J.C., and Cook, N.G.W., 1969, Fundamentals of rock mechanics: London, Methuen and Co., Ltd., 513 p.

Janbu, N., 1973, Slope stability computations, *in* Hirschfield, R.C., and Poulos, S.J., eds., Embankment-dam engineering—Casagrande volume: New York, Wiley, p. 47–86.

Japan Society of Landslide, 1980, Landslides in Japan: Tokyo, The Japan Society of Landslide National Conference on Landslide Control, 44 p.

Kamb, Barclay, 1970, Sliding motion of glaciers—theory and observation: Reviews of Geophysics and Space Physics, v. 8, no. 4, p. 673–728.

_____1986, Stress-gradient coupling in glacier flow—III. Exact longitudinal equilibrium equation: Journal of Glaciology, v. 32, no. 112, p. 335–341.

Kamb, Barclay, and LaChapelle, E., 1964, Direct observation of the mechanism of glacier sliding over bedrock: Journal of Glaciology, v. 5, no. 38, p. 159–172.

Keefer, D.K., 1977, Earthflow: Stanford, Calif., Stanford University, Ph.D. thesis, 317 p.

Keefer, D.K., and Johnson, A.M., 1983, Earth flows—Morphology, mobilization and movement: U.S. Geological Survey Professional Paper 1264, 56 p.

Kenney, T.C., 1968, The influence of mineral composition on the residual strength of natural soils: Proceedings of the Geotechnical Conference, Oslo, Norway, 1967, v. 1, p. 123–129.

Lambe, T.W., and Whitman, R.V., 1969, Soil mechanics: New York, Wiley, 553 p.

Lliboutry, L., 1968, General theory of subglacial cavitation and sliding of temperate glaciers: Journal of Glaciology, v. 7, no. 49, p. 21–58.

Malvern, L.E., 1969, An introduction to the mechanics of a continuous medium: Englewood Cliffs, N.J., Prentice-Hall, 713 p.

Mitchell, J.K., 1976, Fundamentals of soil behavior: New York, Wiley, 422 p.

Mizuno, Keiji, 1989, Landsliding of clayey slopes with a wavy slip surface—Model and its application: Japan, Science Reports of the Institute of Geosciences, University of Tsukuba, sec. A, v. 10, p. 87–151.

Morgenstern, N.R., and Price, V.E., 1965, The analysis of the stability of general slip surfaces: Géotechnique, v. 15, p. 79–93.

Morgenstern, N.R., and Tchalenko, J.S., 1968, Microstructural observations on shear zones from slips in natural clays: Proceedings of the Geotechnical Conference, Oslo, Norway, 1967, v. 1, p. 147–152.

Morland, L.W., 1976a, Glacier sliding down an inclined wavy bed: Journal of Glaciology, v. 17, no. 77, p. 447–462.

_____1976b, Glacier sliding down an inclined wavy bed with friction: Journal of Glaciology, v. 17, no. 77, p. 463–477.

Niigata Laboratory, 1973, Sarukuyoji landslide: Niigata, Japan, Public Works Research Institute of Japan, 15 p. Nye, J.F., 1969, A calculation on the sliding of ice over a wavy surface using a Newtonian viscous approximation: Proceedings of the Royal Society of London, series A, v. 311, p. 445–467.

Nye, J.F., 1969, A calculation on the sliding of ice over a wavy surface using a Newtonian viscous approximation: Proceedings of the Royal Society of London, series A, v. 311, p. 445–467.

_____1970, Glacier sliding without cavitation in a linear viscous approximation: Proceedings of the Royal Society of London, series A, v. 315, p. 381–403.

Palmer, A.C., and Rice, J.R., 1973, The growth of slip surfaces in the progressive failure of over-consolidated clay: Proceedings of the Royal Society of London, series A, v. 332, p. 527–548.

Patton, F.D., 1966, Multiple modes of shear failure in rock and related materials: Urbana, University of Illinois Ph.D. thesis, 293 p.

Prior, D.B., and Stephens, N., 1972, Some movement patterns of temperate mudflows—Examples from northeastern Ireland: Geological Society of America Bulletin, v. 83, no. 8, p. 2533–2543.

Ramiah, B.K., and Purushothamaraj, P., 1971, Influence of strain rate on the residual strength of a kaolinitic clay: Geotechnical Engineering, v. 2, no. 2, p. 151–158.

Rice, J.R. and Cleary, M.P., 1976, Some basic stress diffusion solutions for fluid saturated elastic porous media with compressible constituents: Reviews of Geophysics and Space Physics, v. 14, no. 2, p. 227–241.

Rosenthal, D., 1946, The theory of moving sources of heat and its application to metal treatments: Transactions of the American Society of Mechanical Engineers, v. 68, p. 849–866.

Rybář, Jan, 1968, Ein Beispiel von Bewegsungsmessungen an Rutschungen: Zeitschrift für angewandte Geologie, v. 14, p. 138–141.

Savage, W.Z., and Chleborad, A.F., 1982, A model for creeping flow in landslides: Bulletin of the Association of Engineering Geologists, v. 19, no. 4, p. 333–338.

Savage, W.Z., and Smith, W.K., 1986, A model for the plastic flow of landslides: U.S. Geological Survey Professional Paper 1385, 32 p.

Skempton, A.W., 1954, The pore-pressure coefficients A and B: Géotechnique, v. 4, p. 143–147.

_____1964, Long-term stability of clay slopes: Géotechnique, v. 14, p. 77–102.

Skempton, A.W., Leadbeater, A.D., and Chandler, R.J., 1989, The Mam Tor landslide, North Derbyshire: Philosophical Transactions of the Royal Society of London, series A, v. 329, no. 1607, p. 503–547.

Skempton, A.W., and Petley, D.J., 1968, The strength along structural discontinuities in stiff clays: Proceedings of the Geotechnical Conference, Oslo, Norway, 1967, v. 2, p. 29–48.

Stout, M.L., 1971, Slip surface geometry in landslides, southern California and Norway: Association of Engineering Geologists Bulletin, v. 8, no. 1, p. 59–78.

Suhayda, J.N., and Prior, D.B., 1978, Explanation of submarine landslide morphology by stability analysis and rheological models: Offshore Technology Conference, Proceedings, no. 10, v. 2, p. 1075–1082.

Ter-Stepanian, G., 1965, In-situ determination of the rheological characteristics of soils on slopes, *in* Proceedings of the Sixth International Conference on Soil Mechanics and Foundation Engineering, Montreal, Canada, 1965: Toronto, University of Toronto Press, v. 2, p. 575–577.

Terzaghi, K.V., 1925, Erdbaumechanik auf Bodenphysicalischer Grundlage: Vienna, Franz Deuticke, 399 p.

_____1950, Mechanism of landslides, *in* Paige, Sidney, ed., Application of geology to engineering practice: Geological Society of America, Berkey Volume, p. 83–123.

Wroth, C.P., and Houlsby, G.T., 1985, Soil mechanics—Property characterization and analysis procedures, *in* Proceedings of the Eleventh International Conference on Soil Mechanics and Foundation Engineering, San Francisco, 1985: Rotterdam/Boston, A.A. Balkema, v. 1, p. 1–55.

Wylie, C.R., and Barrett, L.C., 1982, Advanced engineering mathematics: New York, McGraw-Hill, 1,103 p.

Yen, B.C., 1969, Stability of slopes undergoing creep deformation: American Society of Civil Engineers Proceedings, v. 95, no. SM4, p. 1075–1096.

Zaruba, Quido, and Mencl, Vojtech, 1982, Landslides and their control: New York, Elsevier Publishing Co., 324 p.

☆U.S. GOVERNMENT PRINTING OFFICE: 1993-774-049/86029

SELECTED SERIES OF U.S. GEOLOGICAL SURVEY PUBLICATIONS

Periodicals

Earthquakes & Volcanoes (issued bimonthly).
Preliminary Determination of Epicenters (issued monthly).

Technical Books and Reports

Professional Papers are mainly comprehensive scientific reports of wide and lasting interest and importance to professional scientists and engineers. Included are reports on the results of resource studies and of topographic, hydrologic, and geologic investigations. They also include collections of related papers addressing different aspects of a single scientific topic.

Bulletins contain significant data and interpretations that are of lasting scientific interest but are generally more limited in scope or geographic coverage than Professional Papers. They include the results of resource studies and of geologic and topographic investigations; as well as collections of short papers related to a specific topic.

Water-Supply Papers are comprehensive reports that present significant interpretive results of hydrologic investigations of wide interest to professional geologists, hydrologists, and engineers. The series covers investigations in all phases of hydrology, including hydrology, availability of water, quality of water, and use of water.

Circulars present administrative information or important scientific information of wide popular interest in a format designed for distribution at no cost to the public. Information is usually of short-term interest.

Water-Resources Investigations Reports are papers of an interpretive nature made available to the public outside the formal USGS publications series. Copies are reproduced on request unlike formal USGS publications, and they are also available for public inspection at depositories indicated in USGS catalogs.

Open-File Reports include unpublished manuscript reports, maps, and other material that are made available for public consultation at depositories. They are a nonpermanent form of publication that maybe cited in other publications as sources of information.

Maps

Geologic Quadrangle Maps are multicolor geologic maps on topographic bases in 7 1/2- or 15-minute quadrangle formats (scales mainly 1:24,000 or 1:62,500) showing bedrock, surficial, or engineering geology. Maps generally include brief texts; some maps include structure and columnar sections only.

Geophysical Investigations Maps are on topographic or planimetric bases at various scales, they show results of surveys using geophysical techniques, such as gravity, magnetic, seismic, or radioactivity, which reflect subsurface structures that are of economic or geologic significance. Many maps include correlations with the geology.

Miscellaneous Investigations Series Maps are on planimetric or topographic bases of regular and irregular areas at various scales; they present a wide variety of format and subject matter. The series also includes 7 1/2-minute quadrangle photogeologic maps on planimetric bases which show geology as interpreted from aerial photographs. The series also includes maps of Mars and the Moon.

Coal Investigations Maps are geologic maps on topographic or planimetric bases at various scales showing bedrock or surficial geology, stratigraphy, and structural relations in certain coal-resource areas.

Oil and Gas Investigations Charts show stratigraphic information for certain oil and gas fields and other areas having petroleum potential.

Miscellaneous Field Studies Maps are multicolor or black-and-white maps on topographic or planimetric bases on quadrangle or irregular areas at various scales. Pre-1971 maps show bedrock geology in relation to specific mining or mineral-deposit problems; post-1971 maps are primarily black-and-white maps on various subjects such as environmental studies or wilderness mineral investigations.

Hydrologic Investigations Atlases are multicolored or black-and-white maps on topographic or planimetric bases presenting a wide range of geohydrologic data of both regular and irregular areas; the principal scale is 1:24,000, and regional studies are at 1:250,000 scale or smaller.

Catalogs

Permanent catalogs, as well as some others, giving comprehensive listings of U.S. Geological Survey publications are available under the conditions indicated below from USGS Map Distribution, Box 25286, Building 810, Denver Federal Center, Denver, CO 80225. (See latest Price and Availability List.)

"Publications of the Geological Survey, 1879-1961" may be purchased by mail and over the counter in paperback book form and as a set microfiche.

"Publications of the Geological Survey, 1962-1970" may be purchased by mail and over the counter in paperback book form and as a set of microfiche.

"Publications of the U.S. Geological Survey, 1971-1981" may be purchased by mail and over the counter in paperback book form (two volumes, publications listing and index) and as a set of microfiche.

Supplements for 1982, 1983, 1984, 1985, 1986, and for subsequent years since the last permanent catalog may be purchased by mail and over the counter in paperback book form.

State catalogs, "List of U.S. Geological Survey Geologic and Water-Supply Reports and Maps For (State)," may be purchased by mail and over the counter in paperback booklet form only.

"Price and Availability List of U.S. Geological Survey Publications," issued annually, is available free of charge in paperback booklet form only.

Selected copies of a monthly catalog "New Publications of the U.S. Geological Survey" is available free of charge by mail or may be obtained over the counter in paperback booklet form only. Those wishing a free subscription to the monthly catalog "New Publications of the U.S. Geological Survey" should write to the U.S. Geological Survey, 582 National Center, Reston, VA 22092.

Note.–Prices of Government publications listed in older catalogs, announcements, and publications may be incorrect. Therefore, the prices charged may differ from the prices in catalogs, announcements, and publications.